REDUCING CHATTER IN KNIFE-EDGE SCANNING MICROSCOPY

A Thesis

by

RAJ SUNIL SHAH

Submitted to the Office of Graduate and Professional Studies of
Texas A&M University
in partial fulfillment of the requirements for the degree of

MASTER OF SCIENCE

Chair of Committee,	Yoonsuck Choe
Committee Members,	John Keyser
	Louise Abbott
Head of Department,	Dilma Da Silva

December 2014

Major Subject: Computer Science

ABSTRACT

The Knife-Edge Scanning Microscope (KESM) employs a novel form of physical sectioning microscopy: Imaging of tissue while sectioning. KESM was developed in the Brain Networks Lab (BNL) at Texas A&M University. The KESM has been used to section animal tissue embedded in a plastic block using a diamond knife. During each cut, the plastic block containing the tissue contacts the knife and that impact induces vibrations, known as knife chatter. These vibrations introduce noise in the image captured from the cut slice. This research is aimed at determining a metric to quantify knife chatter in the images acquired using the KESM, and to test if the use of a vibrating knife reduces knife chatter.

Knife chatter appears as repeated parallel streaks in the images. A quantitative characterization of knife chatter is difficult since there is no regular pattern with which it appears. Having no regular pattern makes it very challenging to detect the chatter using automated programs. Observing the Fast Fourier Transforms of the images tells us that a narrow vertical band around the central vertical axis contains information exclusively about the chatter, while most of the information about the object in the image is outside the vertical band that represents the knife chatter. Using this information, we can quantitatively characterize knife chatter as a ratio of (1) the width of the region in the Fast Fourier Transform that corresponds to the knife chatter, and (2) the width of the region that corresponds to the object.

Determining if the introduction of vibrations in the KESM diamond knife affects the amount of knife chatter present in the images was achieved by sectioning specimens of nissl-stained zebra-fish embryos embedded into araldite blocks, at different knife vibration frequencies. External sinusoidal wave vibrations were introduced in

the KESM knife from a signal generator throughout the sectioning process. These electrical signals were converted to mechanical waves at the tip of the KESM knife blade. Performing such experiments at different oscillation frequencies enabled us to compare data using the metric described above. The results indicate that sectioning tissues with external vibrations does affect the amount of total data bandwidth taken up just by the chatter, and in some cases, reduces the relative width of the bandwidth taken up by the chatter.

DEDICATION

To Jesus Christ, and my mother

ACKNOWLEDGEMENTS

First and foremost, I dedicate this work to Jesus Christ, who pulled me through it and held me up when I thought I couldn't go on anymore.

I would like to thank my committee chair, Dr. Yoonsuck Choe, and my committee members, Dr. John Keyser, and Dr. Louise Abbott, for their guidance and support throughout the course of this research.

I would like to thank my adviser, Dr. Choe for his generosity, willingness to help me any time I needed it, and for guidance throughout the project.

My lab-mates, Daniel Miller and Wencong Zhang, and my friends, Patrick Lunsford, Jaewook Yoo, and Bhavesh Rathod, provided great help and support during the course of this project.

Thanks also go to my friends and colleagues and the department faculty and staff for making my time at Texas A&M University a great experience.

Finally, thanks to my mother for her constant encouragement and love.

The research reported in this thesis has been supported in part by the National Science Foundation grant#1256086 (PI: Yoonsuck Choe).

NOMENCLATURE

FFT	Fast-Fourier Transform
NSF	National Science Foundation
KESM	Knife-Edge Scanning Microscope
BNL	Brain Networks Laboratory

TABLE OF CONTENTS

Page

LIST OF FIGURES

FIGURE Page

LIST OF TABLES

TABLE Page

1. INTRODUCTION

1.1 Introduction

The process of analyzing the microstructure of biological tissue in three dimensions has proven very helpful in modeling its functionality and understanding the basic mechanisms of life. "Volumetric imaging of tissue at the cellular level, using serial imaging of consecutive tissue sections, provides such ability to acquire microstructures in 3D. Three-dimensional light microscopy in biology uses either optical sectioning or physical sectioning" [1]. Optical sectioning uses a varying focal plane to scan the image of tissues at different depths, whereas physical sectioning cuts the tissue as consecutive serial sections and images them. In either case, images from consecutive planes can be aligned and stacked together to create a 3-D volume from the image data. This 3-D volume can be used to analyze structural aspects of the tissue. The process of optical sectioning has an inherent limitation due to depth resolution issues. Hence, physical sectioning has become a widely employed method to obtain high-resolution volumetric tissue structure data [1].

1.2 Motivation

Each of these 3-D biological microscopy techniques, optical or physical sectioning, has advantages and limitations. The maximum observable thickness of the tissue is restricted in optical sectioning due to the limitations caused by light scattering and diffraction-limited optics. Unfortunately, this also results in a limited Z-axis resolution. It is very difficult to overcome these limitations in optical sectioning [1].

The other method, physical sectioning, destroys the tissue during the sectioning process, and can have cutting-induced noise. Due to some developments and advances, physical sectioning has been gaining a lot of interest in 3-D biological mi-

croscopy. For example, new techniques have been introduced to "concurrently image the tissue while sectioning [12], preserving tissue sections for future analysis [18], and performing multiple immunofluorescence imaging [19]" [1]. These have paved the way for physical sectioning to be the go-to method to obtain high-volume image data from a tissue [17].

A novel technique in physical sectioning microscopy, imaging of the tissue while sectioning, is employed by the Knife-Edge Scanning Microscope (KESM). KESM was developed in the Brain Networks Lab (BNL) at Texas A&M University and has been used to section animal tissue embedded in a plastic block using a diamond knife. During each cut, the plastic block containing the tissue contacts the knife and that impact induces vibrations, known as knife chatter. These vibrations introduce noise in the image captured from the cut slice. Knife chatter usually appears as parallel streaks on the image, which makes it undesirable.

This research is focused on characterizing the knife chatter quantitatively, and develop a technique to reduce it.

1.3 Outline

The rest of the thesis is organized as follows. Chapter 2 provides a general background. Chapter 3 discusses the nature of chatter in KESM. The main technical contents are organized as:

1. Quantitatively characterizing knife chatter (Chapter 4).
2. Reducing the proportion of knife chatter in the images by using a vibrating diamond knife (Chapter 5).
3. Isolating the knife chatter from the image (Chapter 6).

Finally, Chapter 7 discusses contributions and limitations, and concludes the thesis.

2. BACKGROUND

2.1 Physical Sectioning

Physical sectioning methods used for imaging purposes have four principal stages: staining the tissue, embedding it into a polymer block, sectioning it, and imaging it. All of these four steps are independent of each other. The entire block containing the tissue can be stained before the sectioning process. Due to the four steps being independent of each other, this method is a lot slower than optical sectioning, but it gives the ability to use multiple imaging techniques on the same tissue section. The tissue of interest is sectioned into slices of desired thickness. Based on the choice of staining technology and required axial resolution, this is done typically using an ultramicrotome. "Images of successive sections are aligned and stacked in registration to obtain a volumetric data set" [1].

The three stages of staining the tissue, sectioning it, and imaging it limit the speed of the physical sectioning process. "With the advent of high precision machining tools and automation of the cutting process, physical sectioning is emerging as a preferred choice for volumetric imaging of biological tissues. Knife Edge Scanning Microscope (KESM), Automatic Tape-Collecting Lathe-Ultramicrotome (ATLUM), Array Tomography, Serial block-face scanning electron microscopy (SBF-SEM), and Serial section transmission electron microscopy are some of the methods using physical sectioning" [17].

2.2 Knife-Edge Scanning Microscope

The Knife-Edge Scanning Microscope (KESM) (Fig. 2.2) was invented by Bruce H. McCormick and developed by associates in the Brain Networks Laboratory (BNL) at Texas A&M University. It employs a novel technique in light microscopy for

cellular-level volumetric data acquisition. It has been demonstrated that KESM can create cellular data sets of 1 cm^3 in approximately 3 weeks [12]. The instrument is able to volume digitize at 180MB/s a brain specimen embedded in a plastic block. The instrument operates at a sampling frequency of 300nm. It can section a tissue embedded into a plastic block into a three-dimensional mesh of uniform volume elements (voxels). Each voxel is assigned a digital signal amplitude for each optical channel (wavelength) used in scanning the specimen. Physical sectioning is used to circumvent photon-limited image capture (a speed requirement). No deconvolution of the imagery is necessary [2]. An entire mouse brain ($\sim$1 cm^3) can be scanned in less than 100 hours when the KESM is fully operational.

KESM introduces the concept of knife-edge scanning. It not only preserves image registration throughout the depth of the specimen block but also isolates the tissue above the knife from that below to eliminate undesirable events like back-scattering of light and bleaching of fluorescence-stained tissue below the knife. Knife-edge scanning supports all known forms of microscopy (absorption imaging using transmitted light, and reflected light imaging using bright-field, dark-field, DIC, and GFP fluorescence) [2].

The work-piece for the KESM is a tissue embedded into a plastic block (araldite or LR White). It is fixed to a keyed ring. This whole assembly is put into a specimen tank. The specimen tank is filled with water, which is constantly being pumped out so that any floating tissues (slices from previous cuts) do not interfere with the cutting and so that the tissue do not build up on the diamond knife blade. Fig. 2.1 shows the work-piece and the specimen tank.

During the sectioning process, the work piece is moved with the help of three mechanical stages. It is moved against a wedge-shaped stationary diamond knife attached to a knife mount, which is secured to a granite bridge, bolted on to a granite

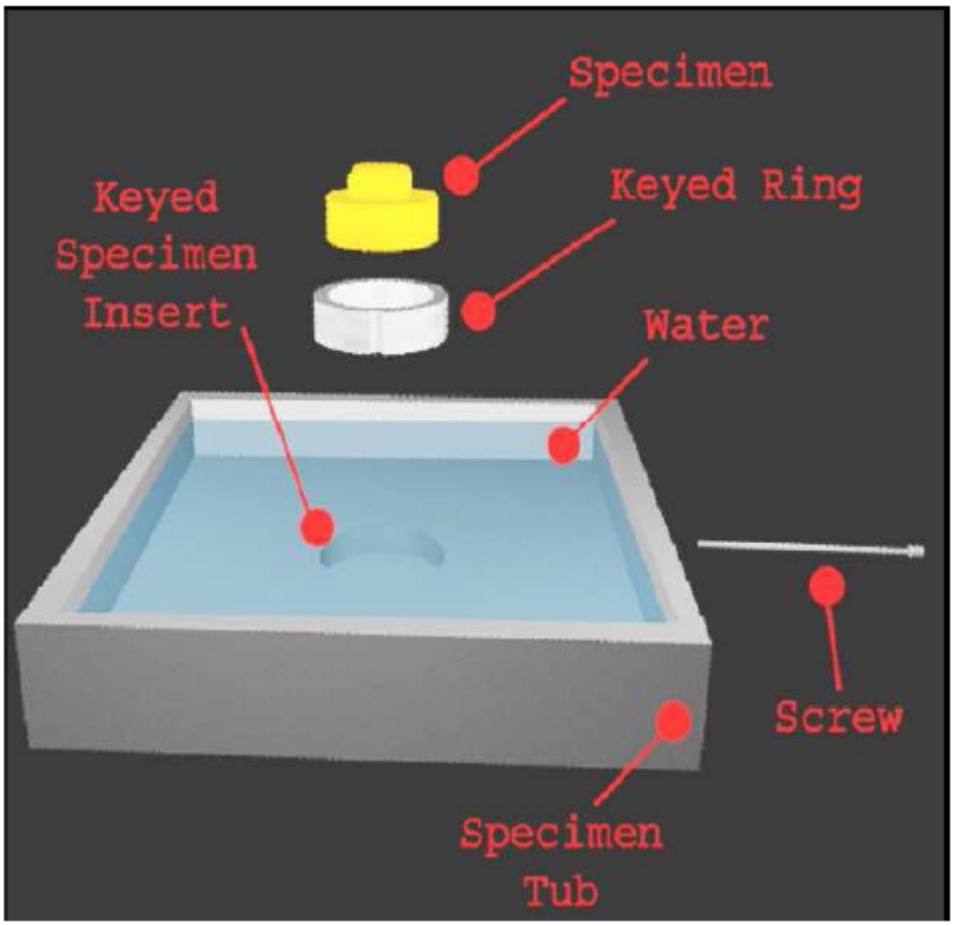

Figure 2.1: KESM work-piece and the specimen tank [16]. This figure is reprinted with permission from "Acquisition and Reconstruction of Brain Tissue Using Knife-Edge Scanning Microscope" by D. M. Mayerich, 2003, M.S. Thesis, Dept of Computer Science, Texas A&M University, © 2003 David Matthew Mayerich.

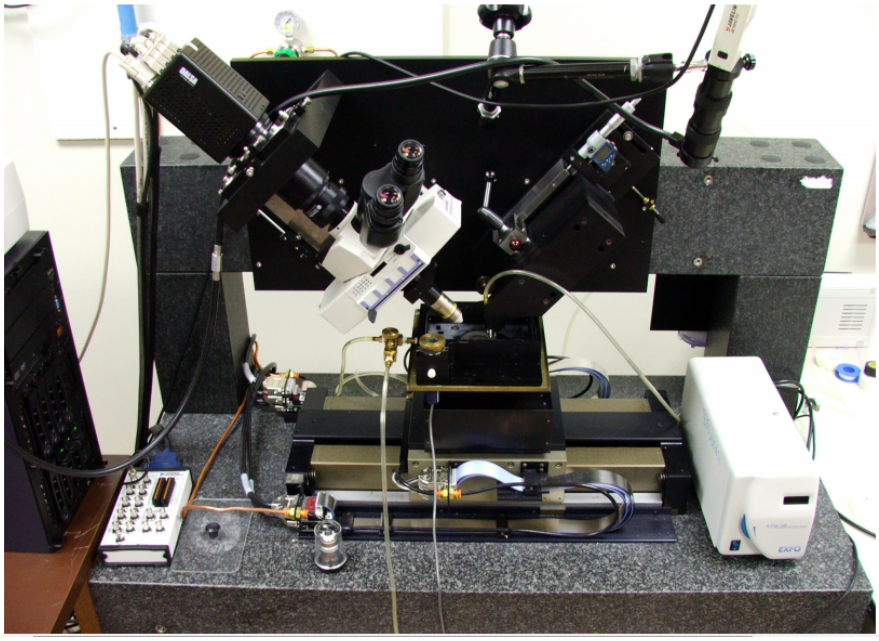

Figure 2.2: Knife-Edge Scanning Microscope [11].

slab. This granite slab also supports the three-axis linear stage. External vibrations are dampened heavily by the granite slab before they reach the system. As mentioned above, imaging is done while sectioning; the cut tissue slice (approximately 15 mm long and 0.5 mm in width) is imaged using a line-scan camera as it rolls over the tip of the top face of the diamond knife (Fig. 2.3). The stage is lowered a little bit, taken back to its original position along the x-axis, and then raised to the height of the new cut. The images are registered in a systematic fashion which enables the reconstruction of the 3-D volume from the images.

2.3 Knife Chatter

The vibrations of the diamond knife in the KESM cause irregular illumination. Knife chatter is a well-known problem in machining [4] [5] [6], but is usually not an issue in imaging. Chatter is a common problem in machining and oscillation cutting mechanism is used to deal with it [13]. KESM uses several mechanical techniques to

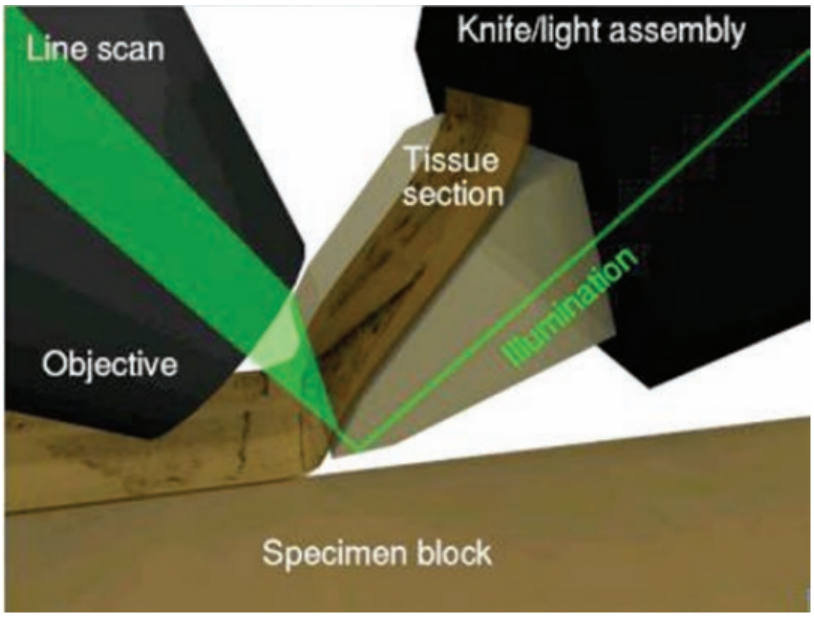

Figure 2.3: KESM Cutting in Progress [12]. This figure is reprinted with permission from "Knife-Edge Scanning Microscopy for Imaging and Reconstruction of Three-Dimensional Anatomical Structures of the Mouse Brain" by Mayerich, David, L. Abbott, and B. McCormick, 2008, Journal of Microscopy 231.1: 134-143, © 2008 The Authors Journal compilation © 2008 The Royal Microscopical Society.

reduce the knife-vibrations: increasing the mechanical stiffness of the specimen and the cutting tool, and cutting at randomized velocities to prevent reinforcement at any frequency. In spite of these measures, the knife chatter is still visible.

KESM cuts as close to the knife-tip as possible as it helps in getting the best alignment possible between different sections, and to ensure that the section is coherent and not warped or torn due to the water current or knife friction. Because the light intensity drops quickly beyond the tip of the knife, these knife vibrations are even more visible. The knife vibration shows up as dark, horizontal stripes along the vertical direction [3]. Fig. 2.4 shows an example of a typical knife chatter. Knife chatter could sometimes result in loss of information.

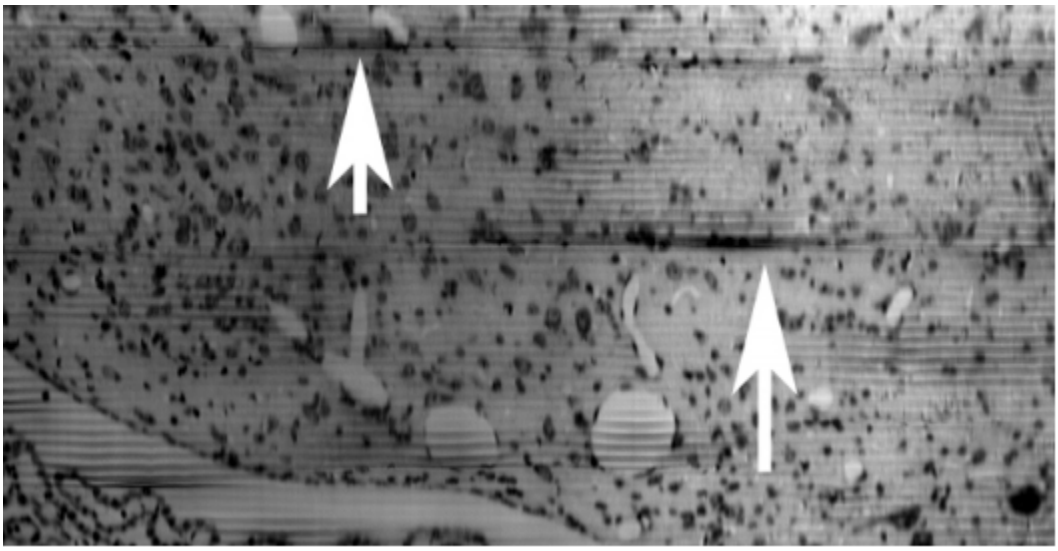

Figure 2.4: Knife Chatter (arrows) [3] © 2007 IEEE.

3. CHATTER IN THE KESM SECTIONING PROCESS

3.1 Introduction

The machining process basically involves sectioning of the work-piece by a relative movement between the work-piece and the cutting tool. This relative motion can induce a variety of vibrations which are undesirable as they could corrupt the smoothness of the cut. One of the most complex ways in which these vibrations manifest is mechanical chatter. They are very difficult to nullify. One other problem is that the chatter is self-sustaining and will continue unless it is stopped. Usually, chatter presents itself as lines or grooves on the surface of the work-piece. An example of this could be seen in Fig. 3.1. It shows the chatter artifacts left on a metal surface during the milling process. Chatter is usually manifested as repeating lines, at regular intervals, based on the frequency of knife-machine vibrations and the cutting speed.

3.2 Types of Chatter

The source of vibration can be used as a differentiating factor between four different types of chatter: frictional, regenerative, mode-coupling, and thermo-mechanical. The four different types of chatter are explained below (see [1] for a review):

1. Frictional chatter: It is caused by the frictional force between the workpiece and the tool flank, or between the section (chip) and the rake surface, or both.

2. Regenerative chatter: It regenerates from the previous cut. When the workpiece is cut over and over at the top surface, this is the most common type of chatter that could appear. It acts like a positive feedback loop because when the cutting tool hits the uneven surface from the previous cut, vibrations are

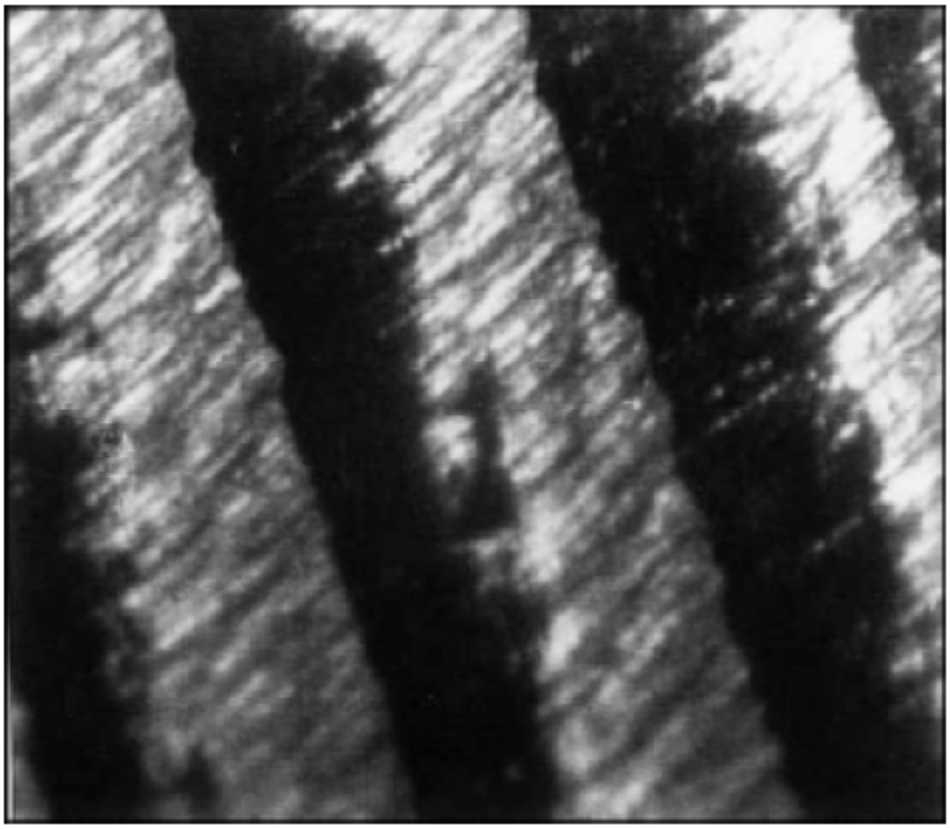

Figure 3.1: Chatter visible as dark bands on the surface of a metal [5]. This figure is reprinted with permission from"Sources of Nonlinearities, Chatter Generation and Suppression in Metal Cutting" by Marian Wiercigroch and Erhan Budak, April 2001, Philosophical Transactions of the Royal Society A: Mathematical, Physical and Engineering Sciences, vol. 359, no. 1781, pp. 663-693, © 2014 The Royal Society.

induced in the cutting tool; and this continues at every step.

3. Mode-coupling chatter: They are caused when the vibration in the cutting force direction induces vibrations in the thrust force direction, or the other way round.

4. Thermo-mechanical chatter: The work-piece material experiences plastic deformation during the cutting process, which in turn leads to changes in strain-rate and temperature. The chatter caused by these changes is called thermo-mechanical chatter.

3.3 Chatter in Physical Sectioning and the KESM

Since the cutting of the specimen and the imaging are done simultaneously in the KESM, vibrations appear as alternating streaks of bright and dark bands on the images. Sometimes, the presence of such chatter artifacts in the images can result in loss of information as the reconstruction algorithm could take in the chatter as something belonging to the object in the image when, in reality, it does not. A solution is to vary the cutting speed and the depth of cutting, but these result in a slower sectioning speed and hence, it would take more time to section the whole volume. Another way to get around this problem is to limit how thin a slice is cut but that would give us a lower z-axis resolution, taking away the advantage that physical sectioning gives. A major type of chatter present in the KESM is the regenerative chatter. When the plastic block housing the tissue comes in contact with the diamond knife, it causes an impact which makes the knife vibrate. These vibrations result in a non-uniform cut over the surface of the block. The subsequent cuts retain a phase-shifted variant of this wavy surface. If it is not stopped, this process keeps on feeding itself [1].

4. QUANTIFYING KNIFE CHATTER IN KESM IMAGES

4.1 Introduction

Chatter typically occurs as parallel stripes orthogonal to the cutting direction. Therefore, there is a frequency associated with the chatter artifacts. If we could look at the frequency spectrum of the image, we could look at frequencies that contribute to the chatter. Discrete-Fourier Transforms (DFTs) are a great way to look at how different data elements appear with different frequencies in the images acquired through the KESM sectioning process. This section explains Discrete-Fourier Transforms, what they mean, how they could be used to quantitatively analyze the chatter in the images, and Fast-Fourier Transforms (FFTs, which are a fast way of computing DFTs).

4.2 Discrete Fourier Transform

Discrete Fourier Transform (DFT) takes as input a finite list of equally spaced samples of a function and converts them into the list of coefficients of a finite combination of complex sinusoids having those same sample values; these complex sinusoids are ordered by their frequencies [7]. It converts the sampled function from its original domain to the frequency domain. In essence, DFTs convert an input function from its domain into the frequency domain.

Consider a discrete one-dimensional signal x(n). It can be thought of as a series of numbers. The signal x(n) can be represented by a sum of many individual frequency components. The DFT can tell us what individual frequencies the signal x(n) is composed of. Figure 4.1a shows an example of how a signal can be broken down into simpler sinusoidal signals.

The DFT of a signal x(n), that has N samples in the series, is given by:

$$X(m) = \sum_{n=0}^{N-1} x(n) * e^{\frac{-j*2*\pi*n*m}{N}} \tag{4.1}$$

Here, j is the square root of -1. The variable m ranges from 0 to N-1 to calculate all the DFT coefficients. It calculates the correlation between the signals x(n) and $e^{\frac{-j*2*\pi*n*m}{N}}$ [14]. But what does it mean to compute this correlation? Before answering that question, let us look at the following equation:

$$e^{-i*\theta} = cos(\theta) - j * sin(\theta). \tag{4.2}$$

Replacing θ with $\frac{2*\pi*n*m}{N}$, we get

$$X(m) = \sum_{n=0}^{N-1} x(n) * (cos(\frac{2 * \pi * n * m}{N}) - j * sin(\frac{2 * \pi * n * m}{N})). \tag{4.3}$$

Using algebra, we can simplify the above equation to,

$$X(m) = \sum_{n=0}^{N-1} x(n) * (cos(\frac{2 * \pi * n * m}{N})) - j * \sum_{n=0}^{N-1} x(n) * (sin(\frac{2 * \pi * n * m}{N})). \tag{4.4}$$

Here, we are computing two different correlations- one between x(n) and a cosine function, and the other between x(n) and a sine function. Now, let us see with an example how this is useful in determining the frequency components of the signal.

For example, consider the following signal:

$$x(t) = sin(2 * \pi * 1000 * t) + 0.5 * sin((2 * \pi * 2000 * t) + (\frac{3 * \pi}{4})) \tag{4.5}$$

For t = 0 to t = 7, our samples are: x(0) = 0.3535, x(1) = 0.3535, x(2) = 0.6464, x(3) = 1.0607, x(4) = 0.3535, x(5) = -1.0607, x(6) = -1.3535, x(7) = -0.3535.

Figures 4.1 and 4.2 show the input signal and the sinusoids at different values of m.

Figure 4.3a shows the spectral content of the example signal.

Thus, using DFT, we can break up a signal into the sinusoidal frequency components that make up the signal. The example above talks about a one-dimensional signal, but the idea of a DFT can be extended to any number of dimensions. For a 2-dimensional matrix (or an image) of size N × N, the equation to calculate the DFT is given by

$$F(u, v) = \frac{1}{MN} \sum_{x=0}^{M-1} \sum_{y=0}^{N-1} f(x, y) e^{-j2\pi(\frac{ux}{M} + \frac{vy}{N})}, \tag{4.6}$$

where f(x,y) is the image in the spatial domain [15].

The idea is that a row is seen as a one-dimensional series, and its DFT is calculated. This is done for all the rows, and then a similar operation is performed on the columns of the transformed image, giving the DFT of the image. The DFT is symmetric, so that the part of the DFT that is to the left of y-axis is reflected on the right of the y-axis, and the part of the DFT above the x-axis is reflected below the x-axis. The axes represent the frequency component values. As we go out further from the origin on the x-axis, the frequency component value increases in either

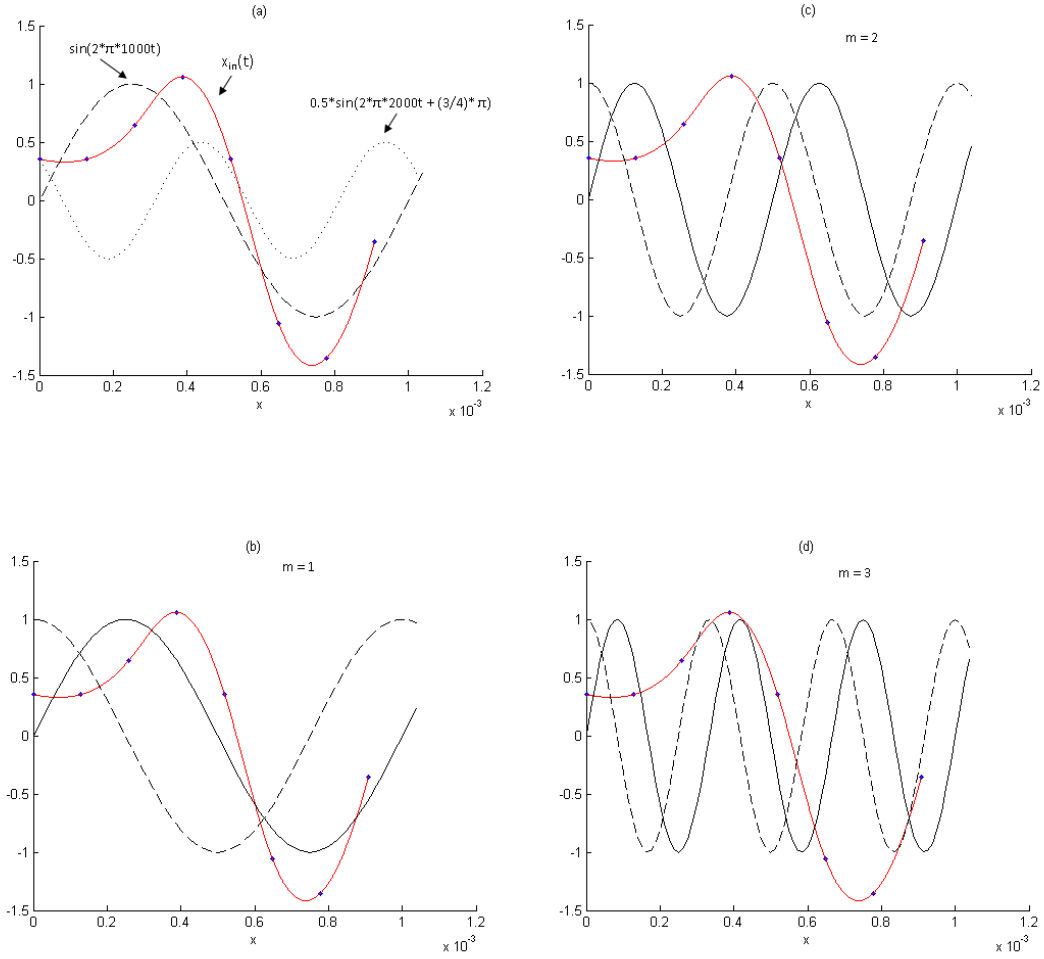

Figure 4.1: DFT of an example signal. (a) the input signal and its constituent sinusoidal signals; (b) the input signal with the m = 1 sinusoids; (c) the input signal with the m = 2 sinusoids; (d) the input signal with the m = 3 sinusoids [14].

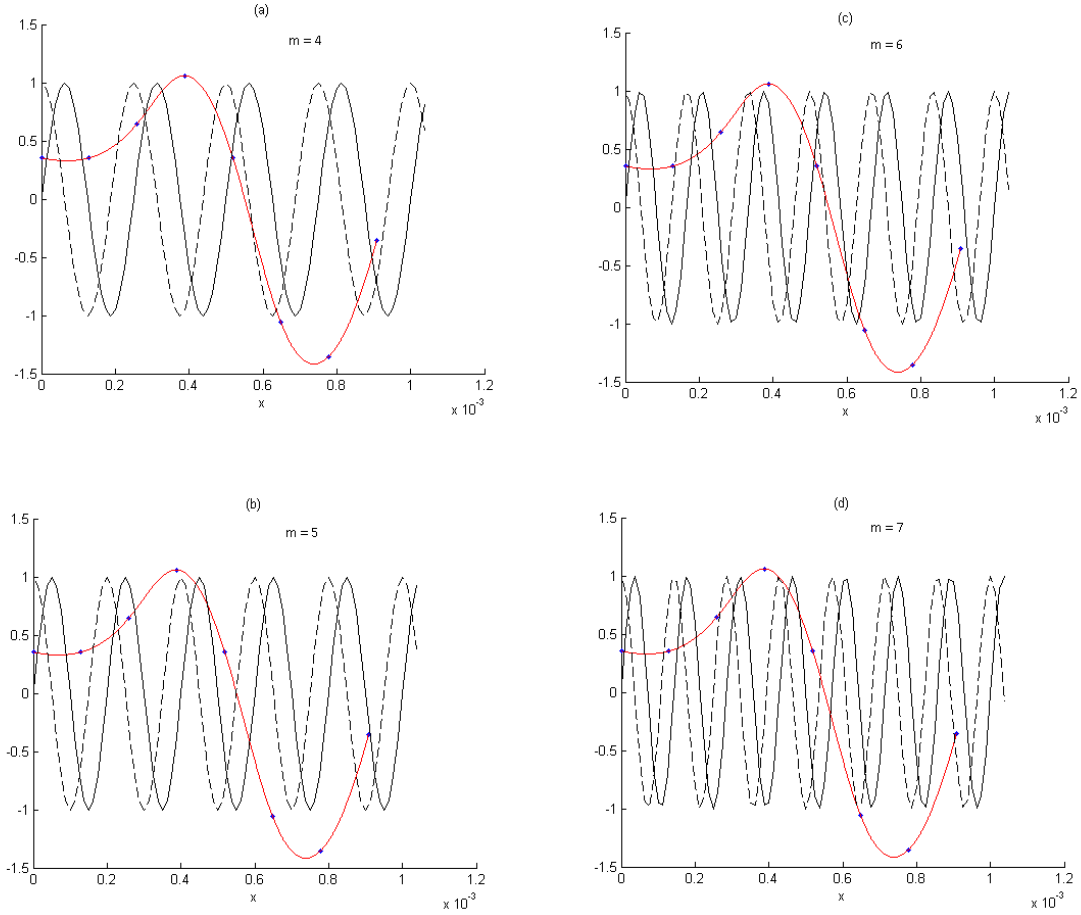

Figure 4.2: DFT of an example signal. (a) the input signal with the m = 4 sinusoids; (b) the input with the m = 5 sinusoids; (c) the input with the m = 6 sinusoids; (d) the input with the m = 7 sinusoids [14].

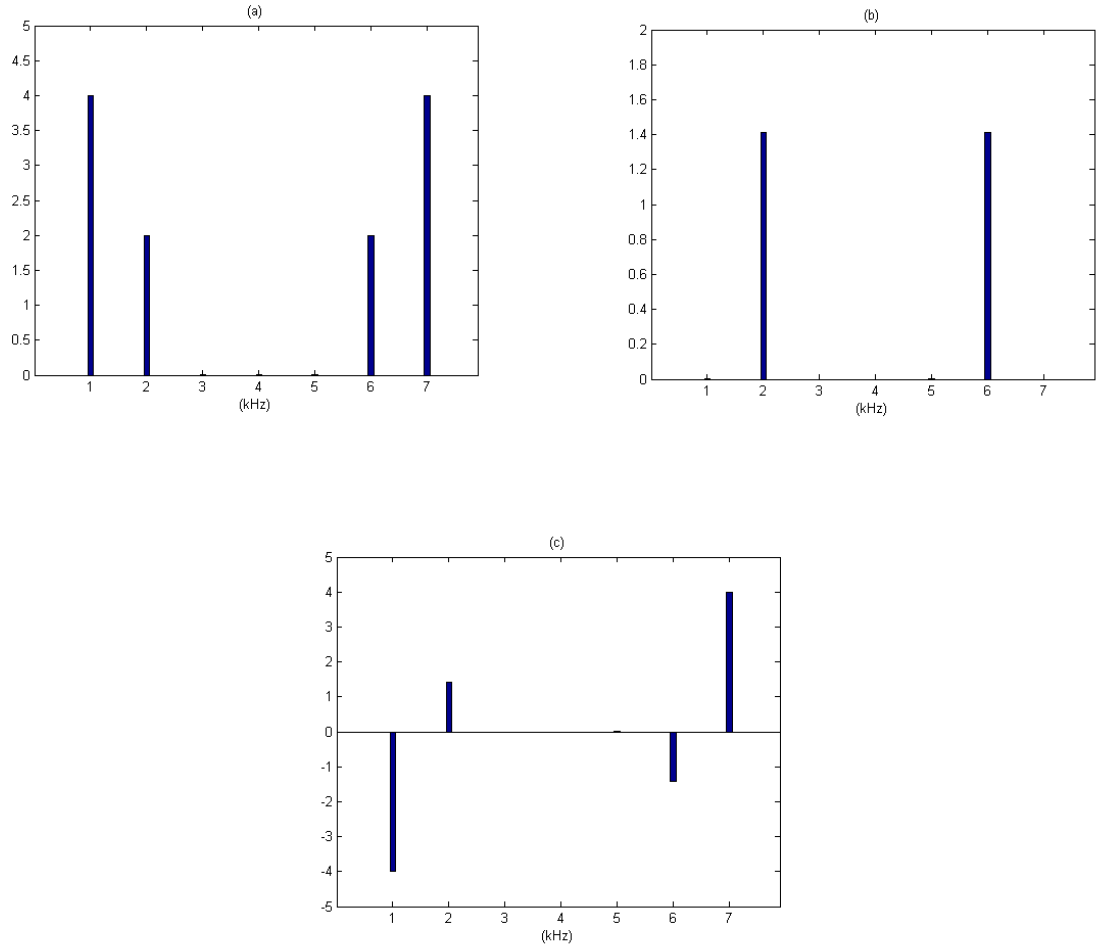

Figure 4.3: DFT of an example signal. (a) magnitude of X(m); (b) real part of X(m); (c) imaginary part of X(m) [14].

direction, and the same is true for the y-axis.

4.3 Fast-Fourier Transform

Fast-Fourier Transform is a fast algorithm to compute the DFT of a function. The above definition for DFT is for a one-dimensional function. Here, we are going to talk about DFTs (or FFTs) of two-dimensional functions. It is a simple extension of the above equation. FFT is used in many image processing applications, such as image analysis, image filtering, image reconstruction, and image compression. The images in the spatial and Fourier domains are of the same size. The DFT of an N $\times$ N 2-dimensional image is given by

$$F(u,v) = \frac{1}{MN} \sum_{x=0}^{M-1} \sum_{y=0}^{N-1} f(x,y) e^{-j2\pi(\frac{ux}{M} + \frac{vy}{N})}, \tag{4.7}$$

where f(x,y) is the image in the spatial domain [15].

The Fast-Fourier transform, when performed on an image, takes the input image and converts it to its frequency domain. The FFT can tell us what frequencies are present in the image.

For example, if we have an image with alternating bands in the horizontal direction as in Figure 4.4, the FFT of that image will have a dot on the x-axis at the frequency value with which the bands in the image alternate. If the bands alternate quicker, the frequency rises and that is reflected in the FFT by a dot at a higher frequency, as shown in Figure 4.5. The FFT is symmetric about the x and the y axes.

Similarly, if there are alternating bands in the vertical direction, the FFT will have dots on the y-axis at values which represent the frequency of the alternating

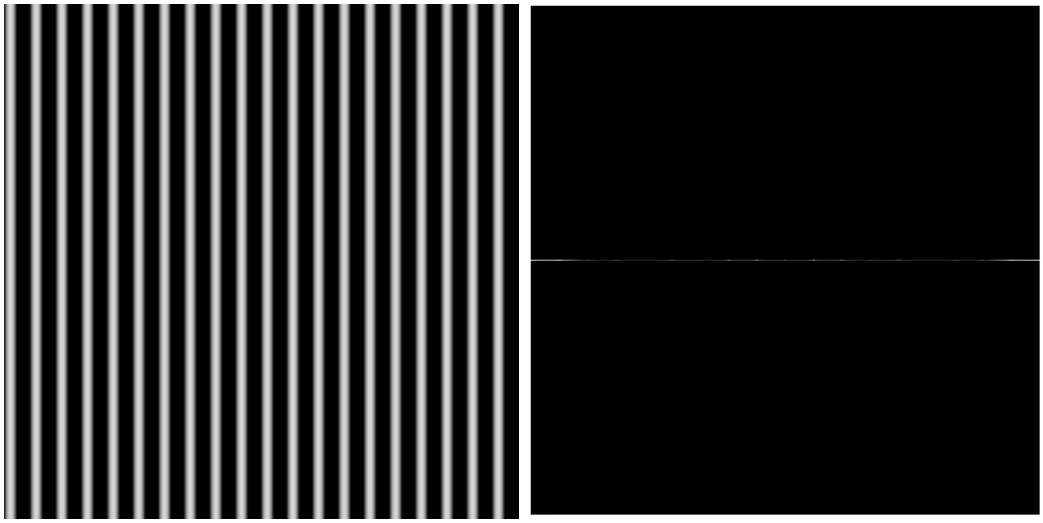

(a) Source Image. (b) Fast-Fourier Transform of (a).

Figure 4.4: Fast- Fourier Transform Example 1. The original FFT's contrast and lighting were changed a little bit so that the dots could be clearly visible.

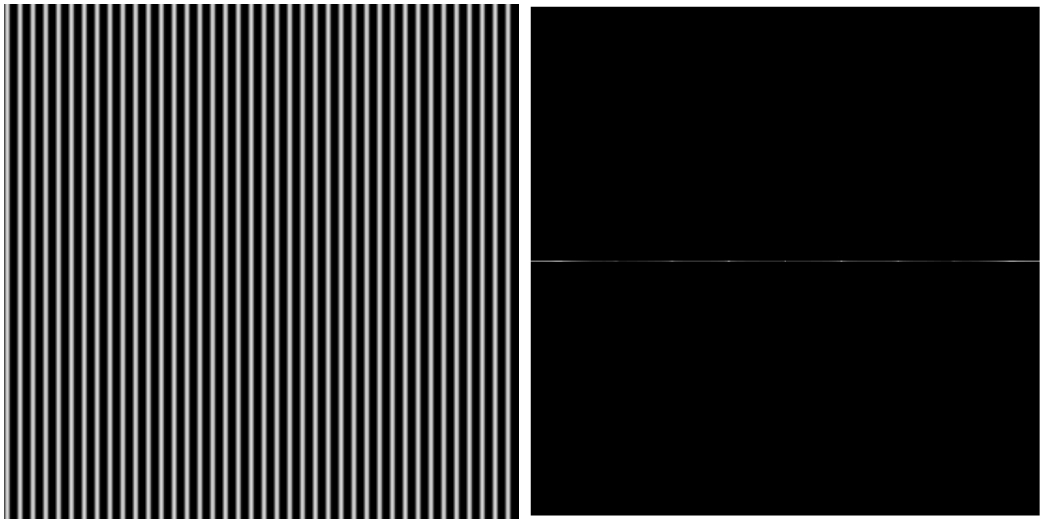

(a) Source Image. (b) Fast-Fourier Transform of (a).

Figure 4.5: Fast- Fourier Transform Example 2. The original FFT's contrast and lighting were changed a little bit so that the dots could be clearly visible.

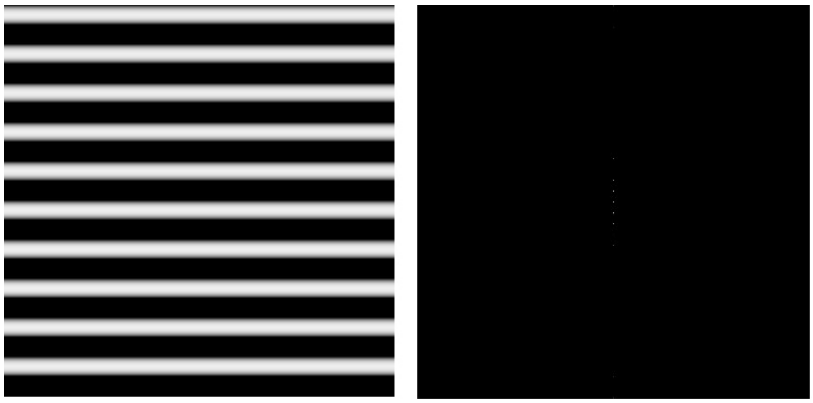

Figure 4.6: Image with alternating bands in the vertical direction and its FFT. The original FFT's contrast and lighting were changed a little bit so that the dots could be clearly visible.

bands. Figure 4.6 shows an example.

A very interesting property of FFTs is that if an inverse FFT operation is performed on the FFT, the result is the original image. So an inverse FFT on Figure 4.4b would give us Figure 4.4a back. As the image gets complex, the FFTs get more and more complicated. Figure 4.7 shows a couple of such examples.

4.4 Nature of Knife Chatter and FFTs

The chatter typically occurs as horizontal stripes in the vertical direction in KESM images. Therefore, there is a frequency associated with the chatter artifacts. Performing FFT on a KESM image shows the frequencies present in the image. Some of the frequency components are there due to the chatter. Therefore, we can use the power spectrum shown in the FFT to figure out the components responsible for the chatter.

A typical image captured using the KESM is shown in Figure 4.8. Only a very small region in the whole image contains an object of interest in this case. The small area of interest is cropped out and shown in Figure 4.9a. It is the eye of a zebrafish embryo. Figure 4.9b shows the cropped image processed for better lighting and

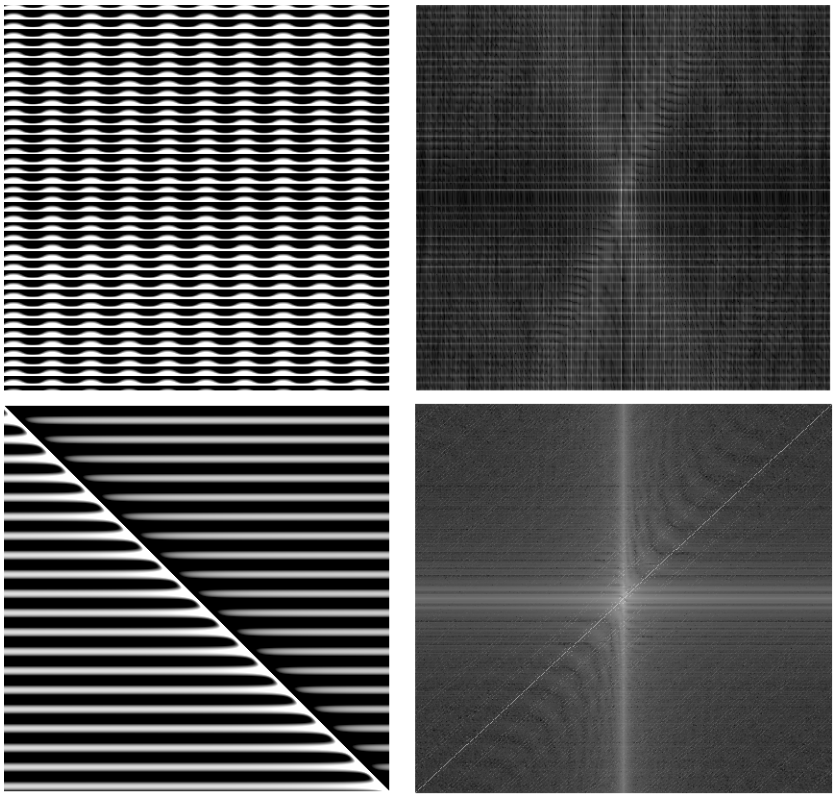

Figure 4.7: Complex images and their respective FFTs.

contrast, along with its FFT in Figure 4.9c.

As it can be seen, most of the data from the image is concentrated around the center. As we move farther out, lesser and lesser information is stored. This is because most of the frequencies present in the image have a low value. To illustrate this, figure 4.11 shows parts of the FFT from figure 4.10 blocked out, and the results of inverse FFT performed on the blocked out FFTs. It is evident that as we increase the width of the unblocked vertical band in the center, the reconstructions from inverse FFT operation get closer and closer to the original image.

4.5 A Quantitative Way to Measure Knife Chatter

It is difficult to quantitatively measure knife chatter. But looking at the FFTs gives us some insight into a way that could help us characterize the knife chatter quantitatively.

Figure 4.11a and Figure 4.11b show that the reconstructions obtained by blocking everything except for a few columns in the center have horizontal streaks where there is knife chatter in the original image. Figure 4.12 shows a KESM image, the reconstructions obtained after blocking everything in the FFT except for 5, 7, and 11 columns in the center along the y-axis. It can be seen that 5 is the maximum number of columns in the center of the FFT that, when left unblocked, give a reconstruction with no hint of the object. We can conclude that just a few vertical bands in the center contain information exclusively about the knife chatter. There is almost no information about the actual object. As we increase the width of this vertical band, we see that the knife chatter becomes clearer and that the object starts appearing, and the reconstructions start getting closer and closer to the original image.

Based on this it seems that the column width in the center responsible for the chatter could be used as a measure of the amount of knife chatter in the image.

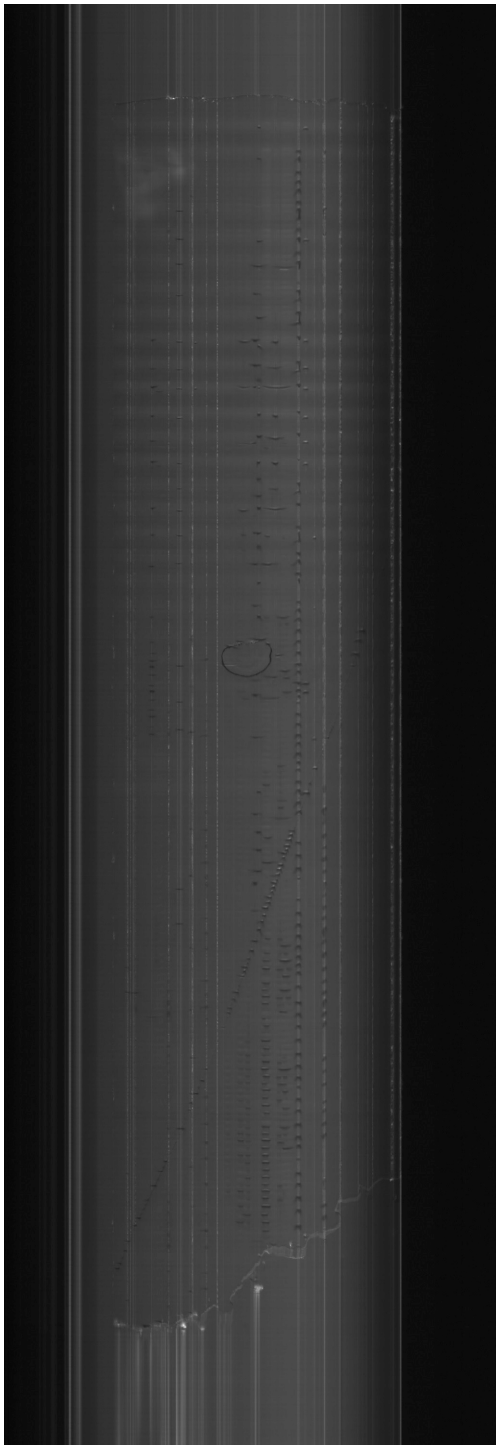

Figure 4.8: Example of a typical image acquired during sectioning using the KESM. This was acquired when sectioning a zebra-fish. The knife was not vibrated.

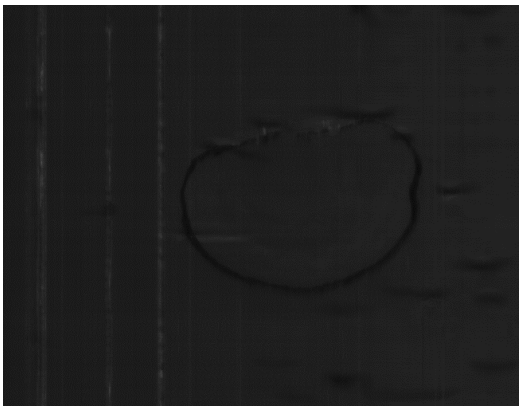

(a) Figure 4.8 cropped so that only the object of interest is prominent.

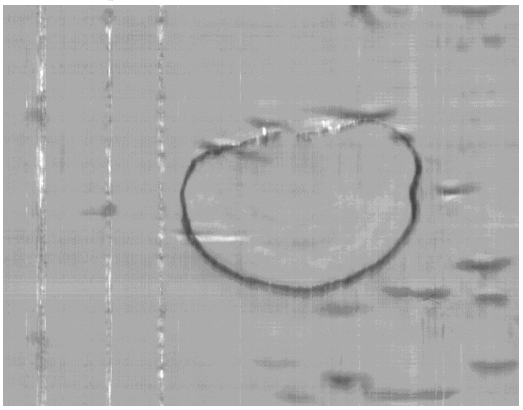

(b) Figure in (a) processed for a better contrast and lighting. The round object is the eye of the zebrafish.

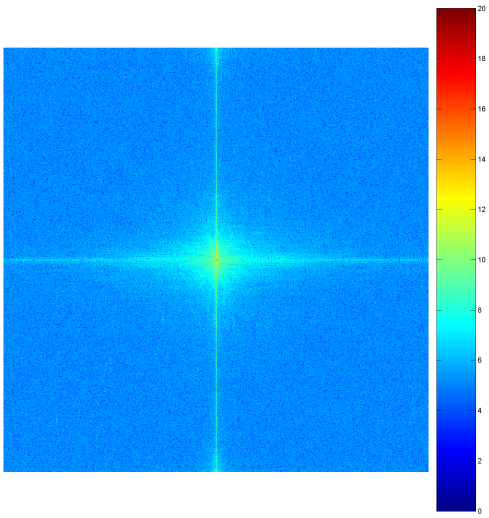

(c) Fast-Fourier Transform of the image in (b).

Figure 4.9: KESM image in Figure 4.8 at various stages of processing.

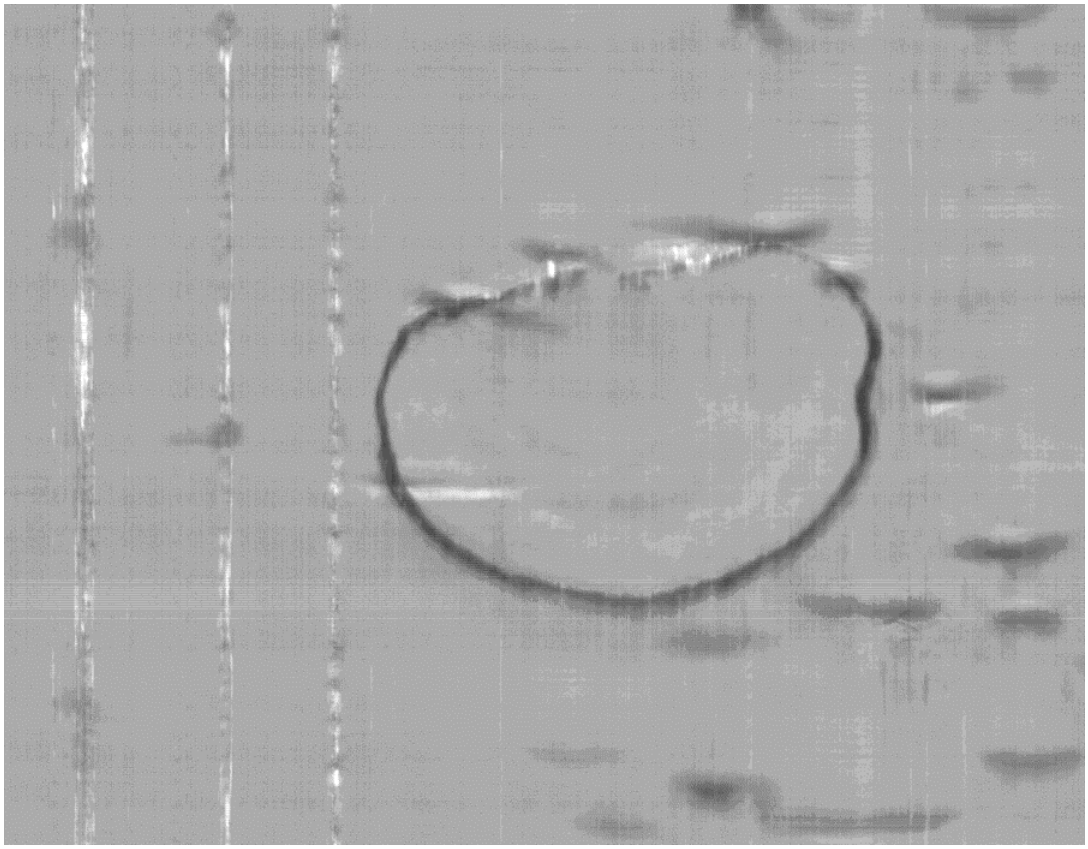

Figure 4.10: A sample image from the KESM data-set. This was acquired when sectioning a zebra-fish. The knife was not vibrated.

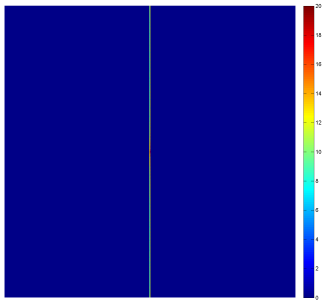

(a) Blocking everything except for the 3 columns in the center.

(b) FFT in (a) reconstructed.

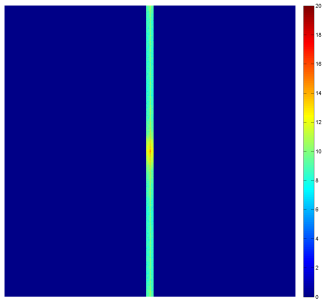

(c) Blocking everything except for the 23 columns in the center.

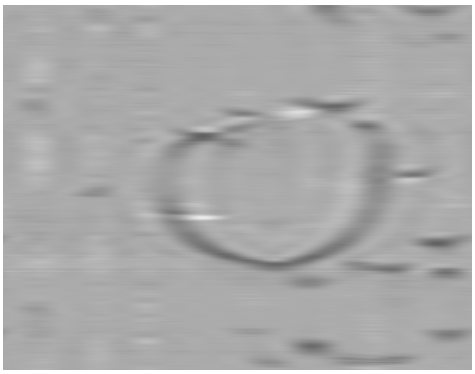

(d) FFT in (c) reconstructed.

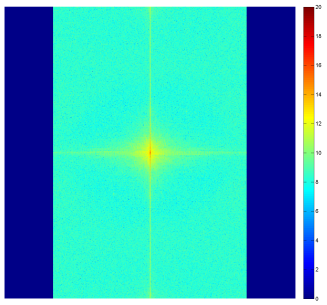

(e) Blocking everything except for the 599 columns in the center.

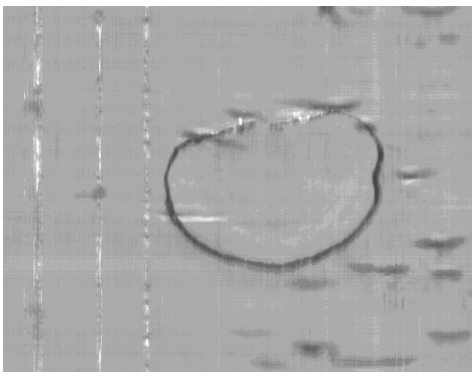

(f) FFT in (e) reconstructed.

Figure 4.11: Parts of the Fourier-Transform of the image in figure 4.10 blocked out, and their corresponding reconstructions.

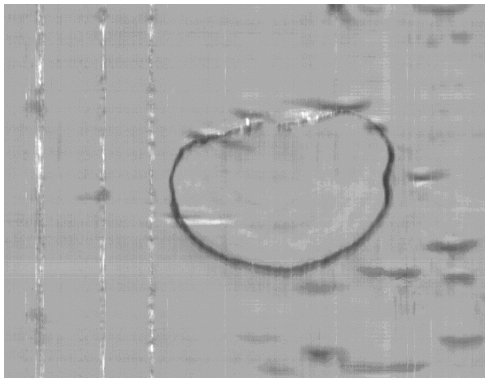

(a) Source Image.

(b) Reconstruction obtained after blocking everything in the FFT except for 5 columns in the center along the y-axis.

(c) Reconstruction obtained after blocking everything in the FFT except for 7 columns in the center along the y-axis.

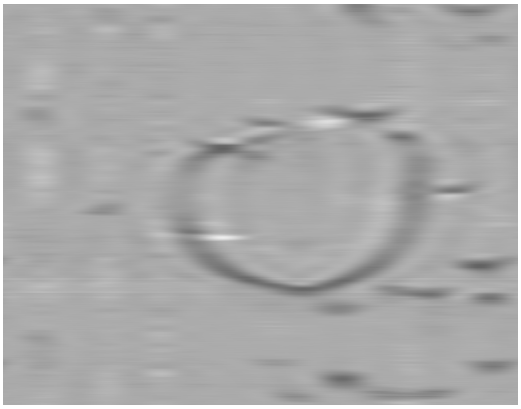

(d) Reconstruction obtained after blocking everything in the FFT except for 11 columns in the center along the y-axis.

Figure 4.12: Example demonstrating the maximum number of columns in the center that when left unblocked give a reconstruction with no hint of the object.

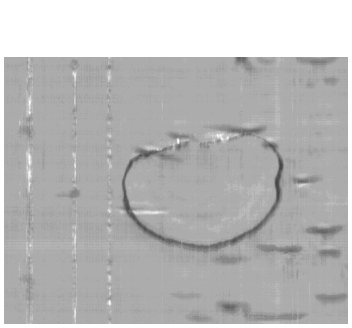

(a) Source Image. Acquired during sectioning zebra-fish embryo without vibrating the knife.

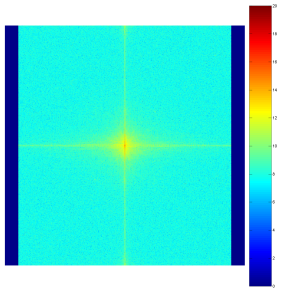

(b) FFT of (a) showing columns left unblocked so that the reconstruction is less than 1 mean pixel difference from the source. Column width = 799.

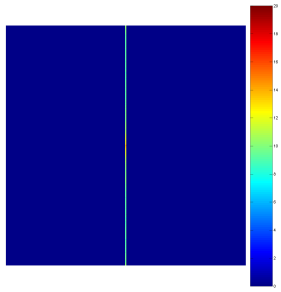

(c) FFT of (a) showing columns left unblocked so that the reconstruction has horizontal streaks in the same location as chatter in the source and no hint of the object. Column width = 5.

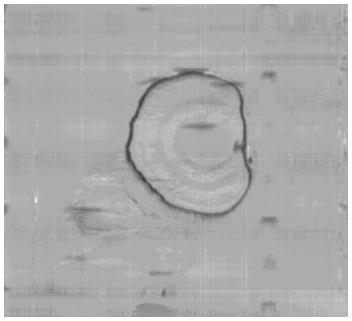

(d) Source Image. Acquired during sectioning zebra-fish embryo while vibrating the knife at 2,500 Hz.

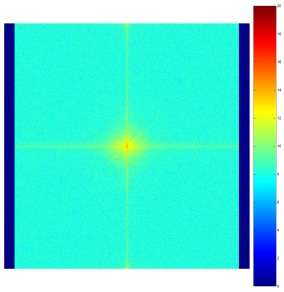

(e) FFT of (d) showing columns left unblocked so that the reconstruction is less than 1 mean pixel difference from the source. Column width = 905.

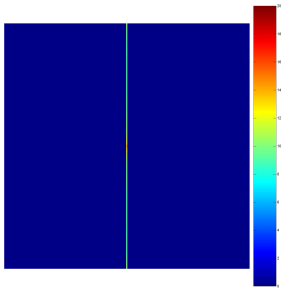

(f) FFT of (d) showing columns left unblocked so that the reconstruction has horizontal streaks in the same location as chatter in the source and no hint of the object. Column width = 5.

Figure 4.13: An example showing that two images with the same chatter bandwidth have different total data bandwidth, and hence different relative amount of chatter.

However, this is not correct because when comparing two images, we also need to take into account the bandwidth of the full image data. We want to know how much of the total data bandwidth is responsible exclusively for chatter. Figure 4.13 illustrates this point. The two images have the same chatter bandwidth (the number of columns in the center responsible for the chatter) but different bandwidths for the total image data, and hence have different relative amount of knife chatter.

We need to find out the total data bandwidth, which means that we need to

Number of center columns in the FFT left unblocked	Mean Pixel Distance Between the Source and the Reconstruction
5	7.6895
23	6.2136
179	4.3995
419	3.7219
719	2.4123
899	0.2088

Table 4.1: Mean pixel distances for the image in Figure 4.14.

find out how many columns in the center of the FFT should we keep unblocked so that the reconstruction is very close to the source image. But before we do that, we need to have a way to measure similarity between the reconstruction and the source image. One way to measure similarity between two images is to calculate the mean pixel distance between the images. Table 4.1 shows the widths of the vertical bands in the center of the FFT that are not blocked out, and the mean pixel distance between the reconstructions obtained from the blocked-out FFTs and the original image (Figure 4.14). It can be seen that the mean pixel distance reduces as we block less and less of the FFT. This means that most of the information about the object and the chatter should be contained in the reconstruction that is 1 or less mean pixel distance away from the original image.

A ratio of two numbers, (1) the width of the unblocked vertical band in the FFT whose reconstruction gives us the horizontal chatter streaks but no object information, and (2) the width of the unblocked vertical band in the FFT whose reconstruction is 1 or less mean pixel distance away from the original image, can tell us how much of the frequency spectrum of the image is exclusively occupied by knife chatter. Since less knife chatter is desirable, the smaller this ratio, the better. The following equation captures this idea and shows how to calculate the percentage of the total

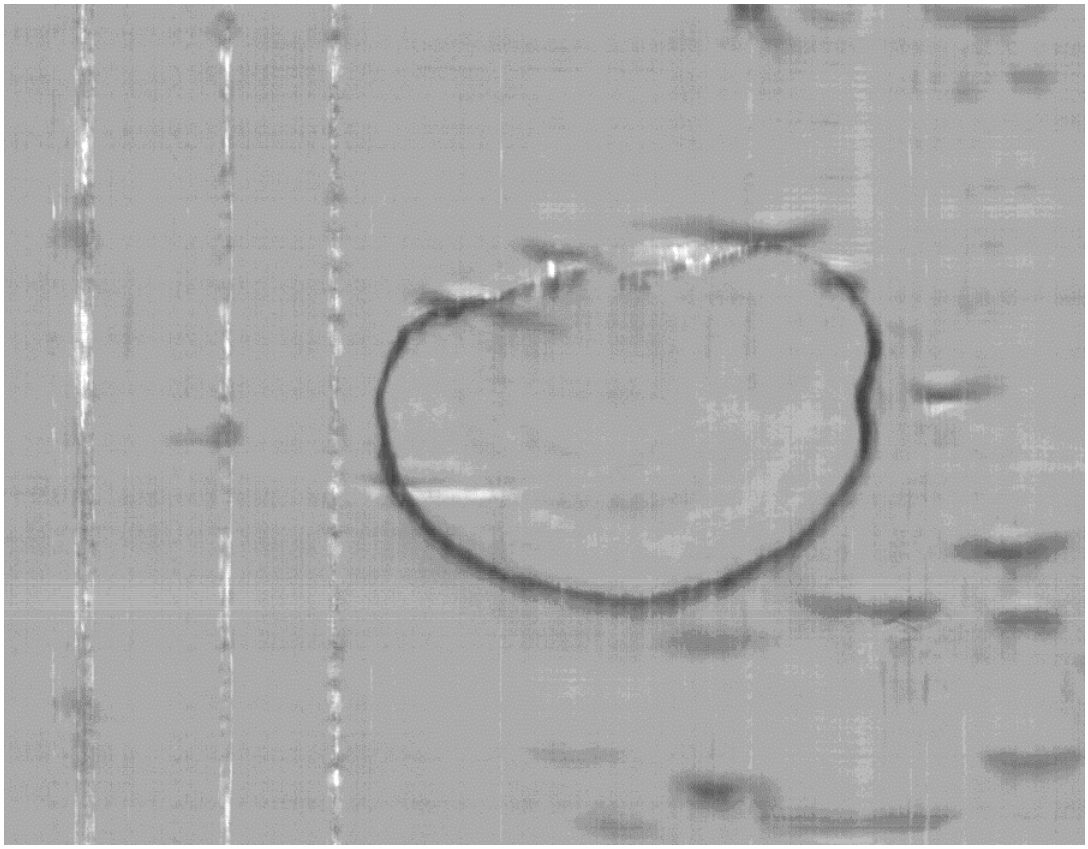

Figure 4.14: A sample image from the KESM data-set. This was acquired when sectioning a zebra-fish. The knife was not vibrated.

image data bandwidth responsible for knife chatter:

$$Proportion\,of\,Knife\,Chatter = \frac{Chatter\,Bandwidth}{Image\,Data\,Bandwidth}, \tag{4.8}$$

where, "Chatter Bandwidth" is the maximum number of columns along the vertical y-axis in the FFT, that when left unblocked while everything else is completely blocked out, give a reconstruction having horizontal streaks in the same places as there is knife chatter in the original image, and "Image Data Bandwidth" is the minimum number of columns along the vertical y-axis in the FFT that, when left unblocked while everything else is completely blocked out, gives a reconstruction that is equal to or less than 1 mean pixel difference from the source image. Here, completely blocking out a column means setting all its elements (rows) to zero value. In the results section, this ratio is used to compare different sets of images.

The bandwidth responsible for the chatter is determined manually, in an iterative manner. During each iteration, the number of columns blocked on either side of y-axis is reduced by 1 and the result displayed on the screen. This process continues until there is a hint of the object in the reconstruction. This column width is recorded.

The process of determining the column width at which the reconstruction has 1 or less mean pixel difference from the source can be automated. The images in Figure 4.15 show the original image, the corresponding FFT, and the blocked out regions of the FFT corresponding to the two criteria. The noise-to-data ratio for this image was 0.006257822.

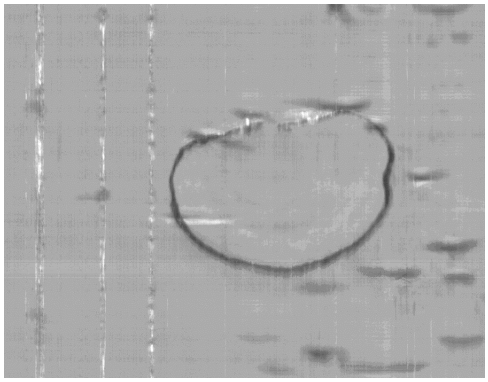

(a)

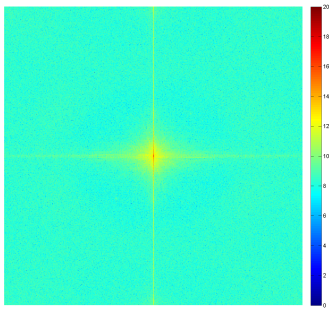

(b)

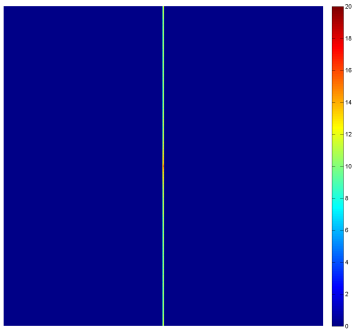

(c)

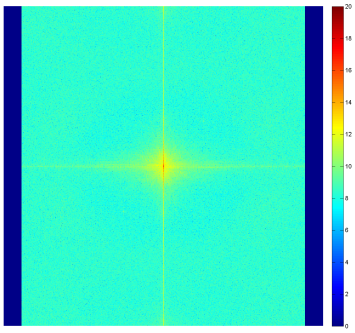

(d)

Figure 4.15: A demonstration of the the chatter-to-total data ratio. (a) Source Image. (b) FFT of (a). (c) FFT of (a) after blocking out everything but 5 columns in the center of the FFT, to have streaks in the reconstruction where there is knife chatter in the original image. (d) FFT of (a) after blocking out everything but 799 columns in the center of the FFT, to have a reconstruction with a mean pixel distance of less than 1 from the source image.

5. REDUCING CHATTER USING A VIBRATING KNIFE

5.1 Introduction

Knife chatter can be reduced by vibrating the diamond knife. The vibration is generated by a piezoelectric oscillator integrated into the knife. When the vibrating knife is fed an external electrical signal as input, the piezoelectric oscillator vibrates the knife parallel to the cutting edge. Vibrating diamond knife was invented by Studer and Gnaegi to minimize the compression in the ultrathin sectioning of the polymer [8]. While sectioning with a vibrating knife, since the volume of the section remains the same, the section becomes thinner at the same depth of cut due to increase in the length of the stroke [1].

5.2 Using a Vibrating Knife to Reduce the Relative Amount of Knife Chatter

To determine if using a vibrating knife would reduce the relative amount of knife chatter in an image, as described in the last chapter, a series of experiments were conducted. Each experiment involved sectioning a zebra-fish embryo using the vibrating knife, either without any input frequency or with a constant frequency throughout the sectioning process.

The goal was to see how the relative amount of knife chatter, as described by the ratio discussed in the last chapter, varies among the images obtained in such a manner. A desirable result is a decrease in the ratio, when a certain frequency was used.

5.3 Methods and Experiments

I conducted several experiments (involving sectioning of nissl-stained zebra-fish embryos), each with a different input frequency to the vibrating knife. The exper-

iments reported in this thesis were conducted at frequencies of 2,500 Hz, 7,500 Hz, and 10,500 Hz. We also conducted a few experiments without vibrating the knife, one of which is reported in this thesis.

The volumetric image data obtained from these experiments were very raw. It had to be processed to be able to compare images from different experiments. Also, from the images obtained during the sectioning process, only few have any object information in them. Such images were culled out from the entire collection. The object information in a typical image is very less compared to the size of the image. The irrelevant information was cropped out so the object information is prominent.

To compare images from different experiments, four test cases were designed. Each test case had a sample image from experiments conducted without vibrating the knife, and vibrating the knife at frequencies of 2,500 Hz, 7,500 Hz, and 10,500 Hz. The sample images were hand-picked from the image set at random by the experimenter (myself). All the images were processed so that the images in one test case have a similar contrast and lighting.

Fast Fourier Transforms for all the images were computed using MATLAB's fast-fourier transform function. To determine the proportion of chatter frequencies in each image, the vertical frequency band in the center that had information exclusively about the chatter was determined by starting with a Fourier Transform of the image completely blocked out, and then unblocking 2 columns, one on each side of and at an equal distance from the central vertical line, until the reconstructions showed any hint of the object. This band was widened and the reconstructions were compared against the original image until the mean pixel difference was 1 or less. This provided all the information needed to calculate the relative amount of chatter bandwidth in all the images. The following pages present the images and the results obtained in the test cases.

The results of the four test cases are reported in Tables 5.1 through 5.4. Table 5.5 contains the average of the results from all the experiments. Figures 5.1 to 5.16 show the test case images, their FFTs, and the reconstructions.

	Leftmost unblocked column for chatter	Rightmost unblocked column for chatter	Leftmost unblocked column for all data	Rightmost unblocked column for all data	Width of chatter band	Width of data band	Ratio (Equation 4.8)
No Vibrations	-3	3	-400	400	5	799	0.006257822
2,500 Hz	-3	3	-453	453	5	905	0.005524862
7,500 Hz	-3	3	-402	402	5	803	0.00622665
10,500 Hz	-2	2	-304	304	3	607	0.004942339

Table 5.1: Results for test-case 1.

	Leftmost unblocked column for chatter	Rightmost unblocked column for chatter	Leftmost unblocked column for all data	Rightmost unblocked column for all data	Width of chatter band	Width of data band	Ratio (Equation 4.8)
No Vibrations	-3	3	-398	398	5	795	0.006289308
2,500 Hz	-2	2	-358	358	3	715	0.004195804
7,500 Hz	-3	3	-395	395	5	789	0.006337136
10,500 Hz	-2	2	-305	305	3	609	0.004926108

Table 5.2: Results for test-case 2.

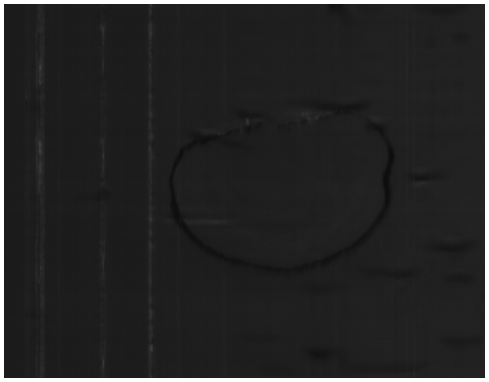

(a) Original.

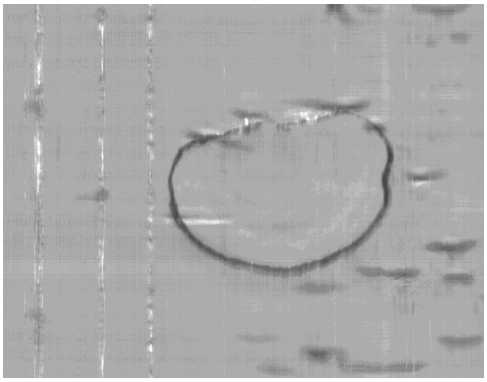

(b) Cleaned.

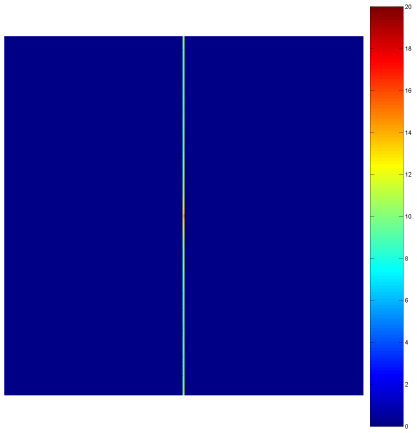

(c) FFT with the Chatter Data Band.

(d) Reconstruction of (c).

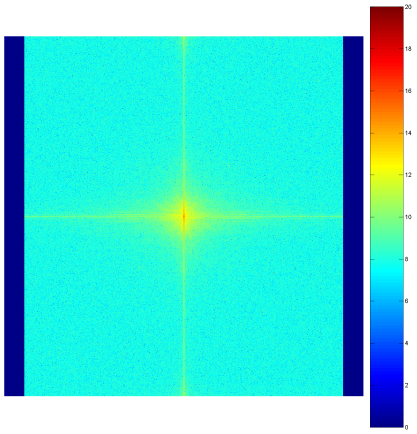

(e) FFT with the Whole Image Data Band.

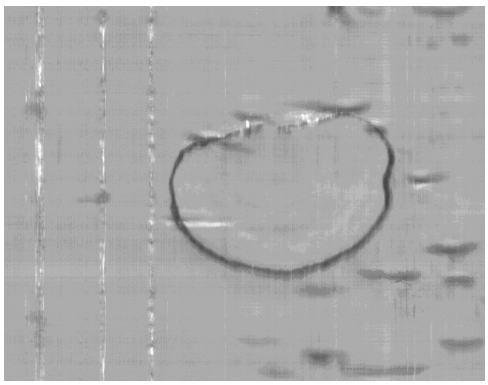

(f) Reconstruction of (e).

Figure 5.1: Image data collected while vibrating the knife at no frequency for the first test-case.

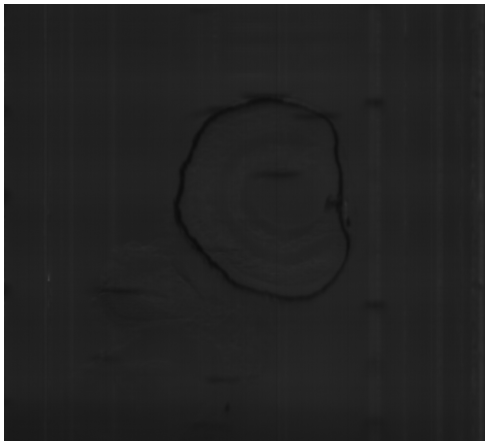

(a) Original.

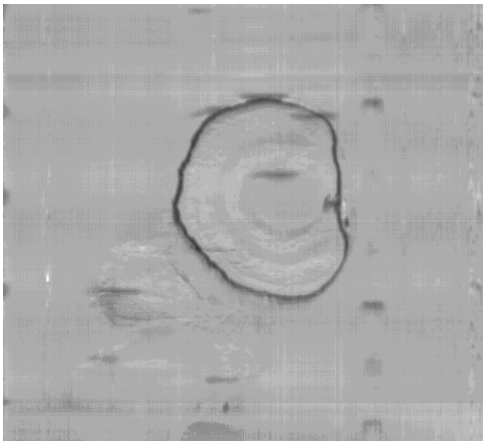

(b) Cleaned.

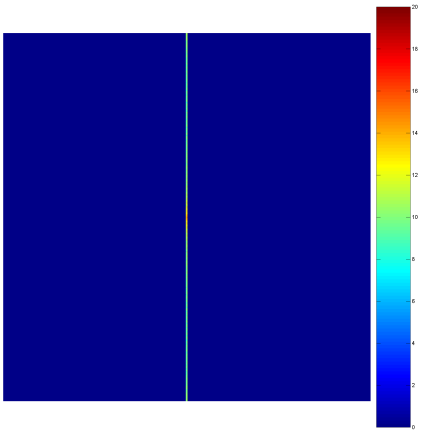

(c) FFT with the Chatter Data Band.

(d) Reconstruction of (c).

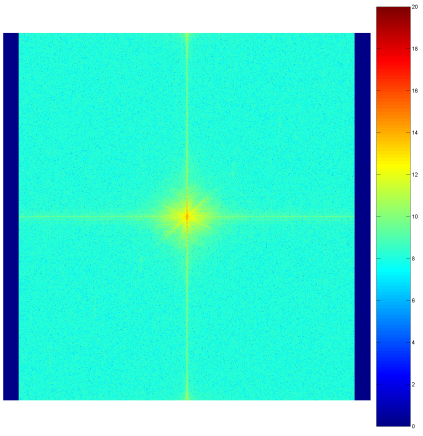

(e) FFT with the Whole Image Data Band.

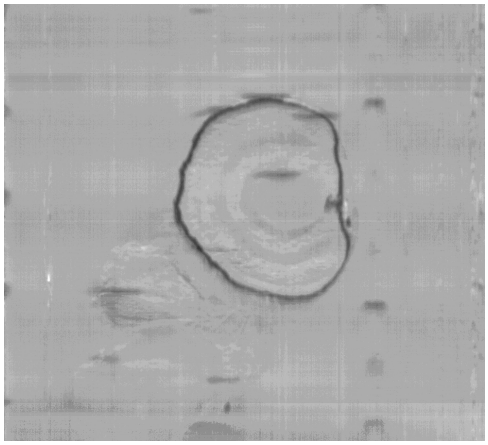

(f) Reconstruction of (e).

Figure 5.2: Image data collected while vibrating the knife at 2,500 Hz frequency for the first test-case.

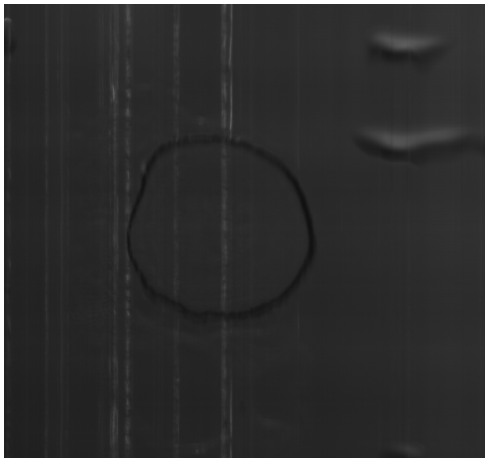

(a) Original.

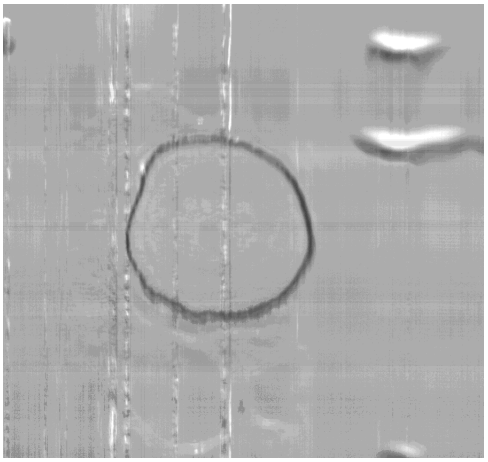

(b) Cleaned.

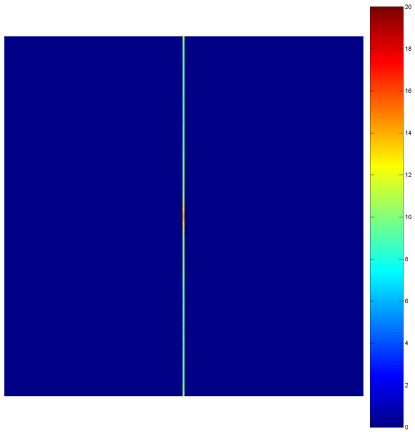

(c) FFT with the Chatter Data Band.

(d) Reconstruction of (c).

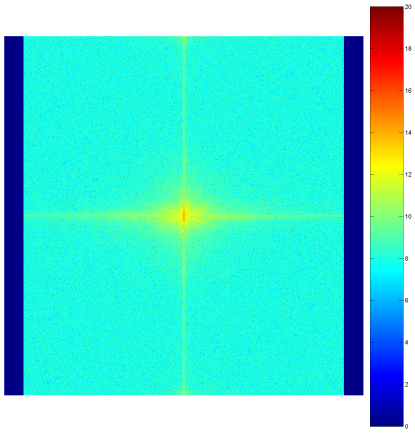

(e) FFT with the Whole Image Data Band.

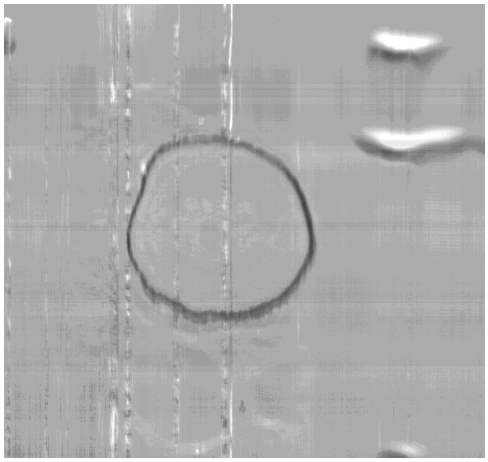

(f) Reconstruction of (e).

Figure 5.3: Image data collected while vibrating the knife at 7,500 Hz frequency for the first test-case.

(a) Original.

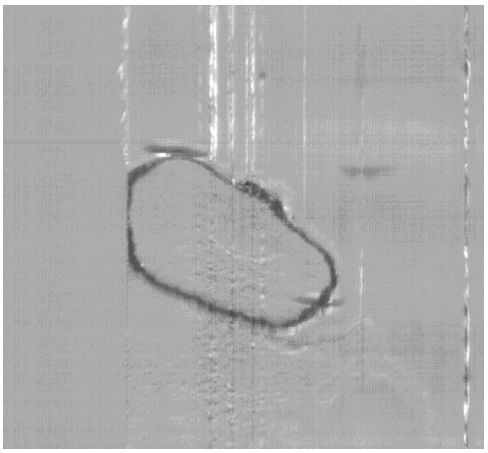

(b) Cleaned.

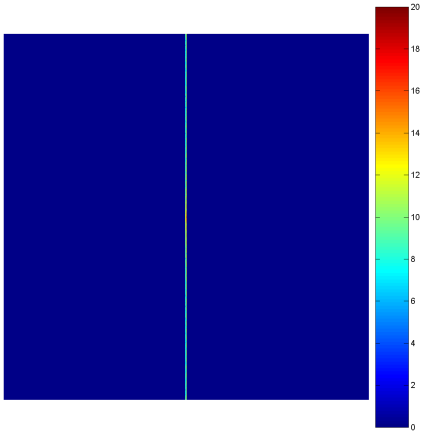

(c) FFT with the Chatter Data Band.

(d) Reconstruction of (c).

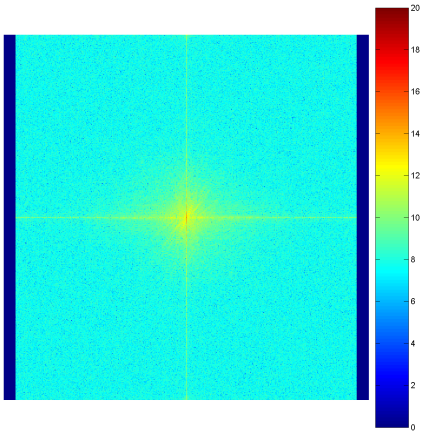

(e) FFT with the Whole Image Data Band.

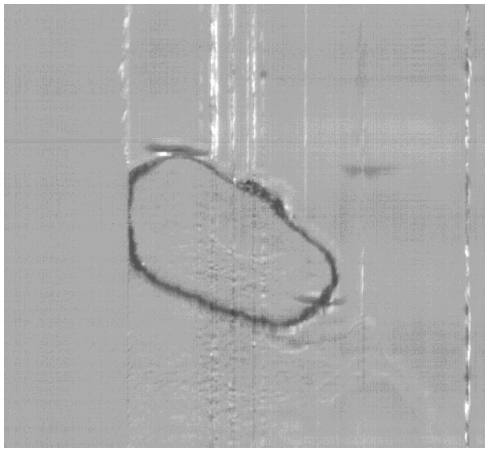

(f) Reconstruction of (e).

Figure 5.4: Image data collected while vibrating the knife at 10, 500 Hz frequency for the first test-case.

(a) Original.

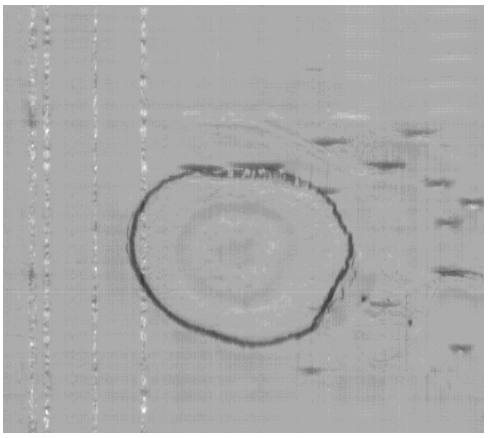

(b) Cleaned.

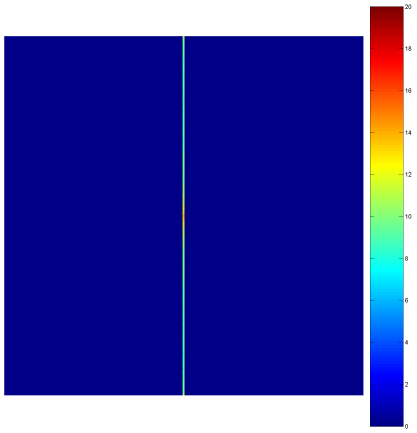

(c) FFT with the Chatter Data Band.

(d) Reconstruction of (c).

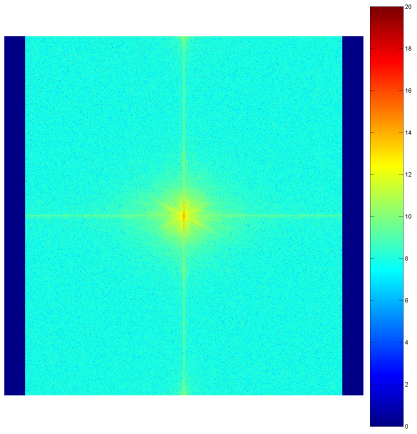

(e) FFT with the Whole Image Data Band.

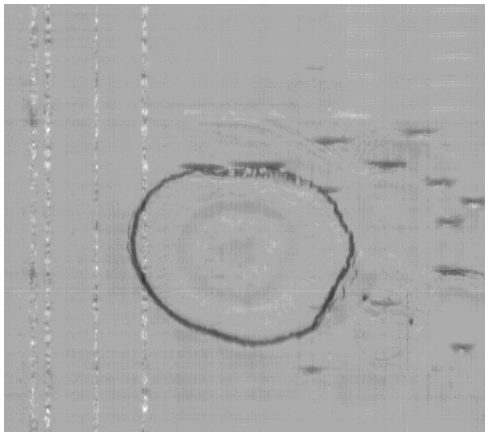

(f) Reconstruction of (e).

Figure 5.5: Image data collected while vibrating the knife at no frequency for the second test-case.

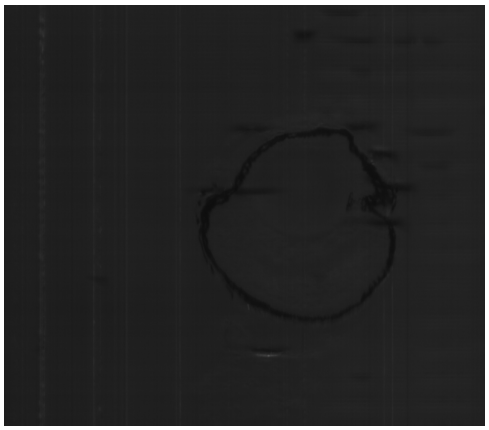

(a) Original.

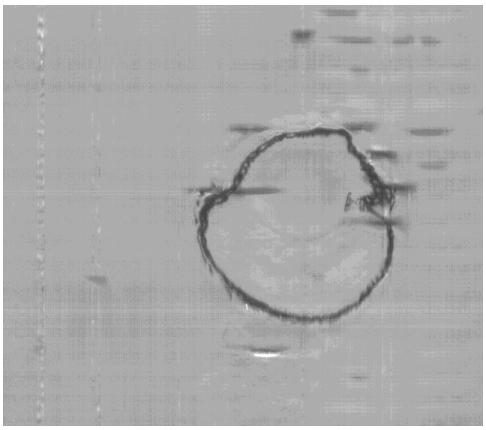

(b) Cleaned.

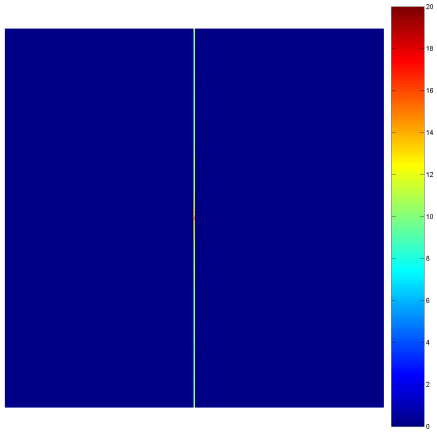

(c) FFT with the Chatter Data Band.

(d) Reconstruction of (c).

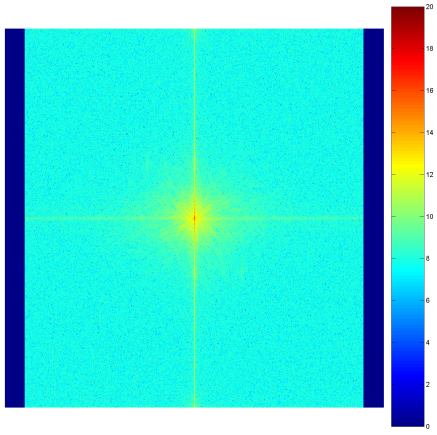

(e) FFT with the Whole Image Data Band.

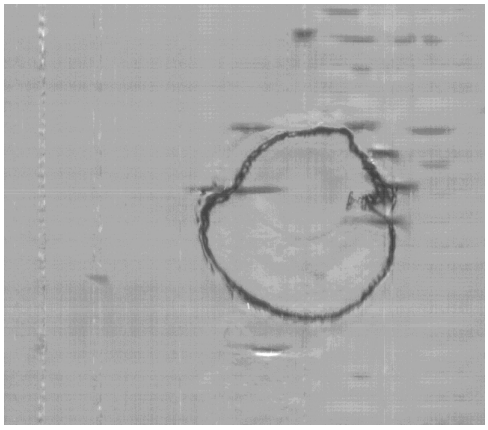

(f) Reconstruction of (e).

Figure 5.6: Image data collected while vibrating the knife at 2,500 Hz frequency for the second test-case.

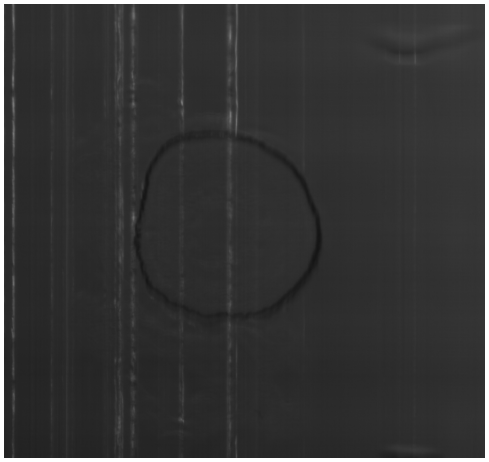

(a) Original.

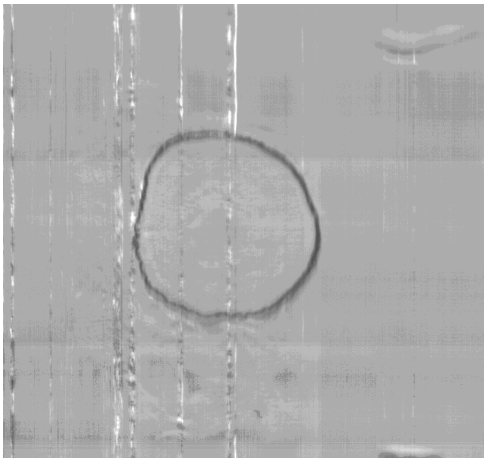

(b) Cleaned.

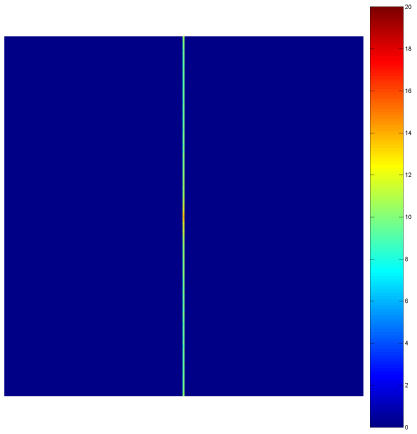

(c) FFT with the Chatter Data Band.

(d) Reconstruction of (c).

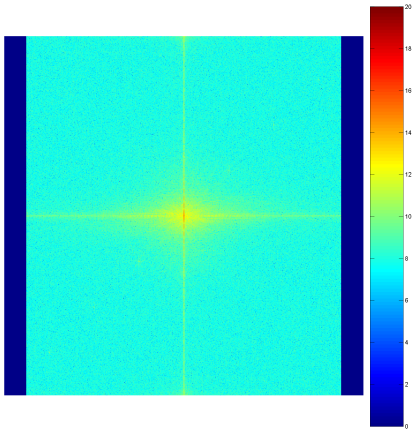

(e) FFT with the Whole Image Data Band.

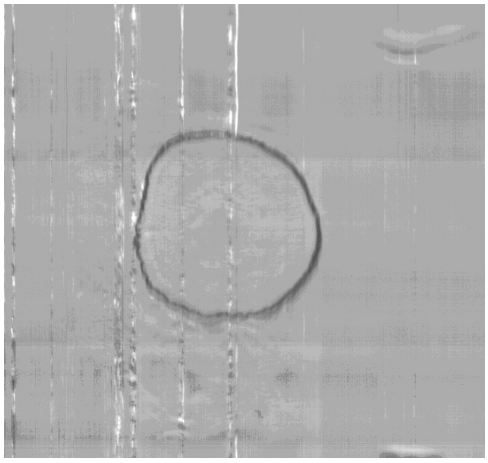

(f) Reconstruction of (e).

Figure 5.7: Image data collected while vibrating the knife at 7,500 Hz frequency for the second test-case.

(a) Original.

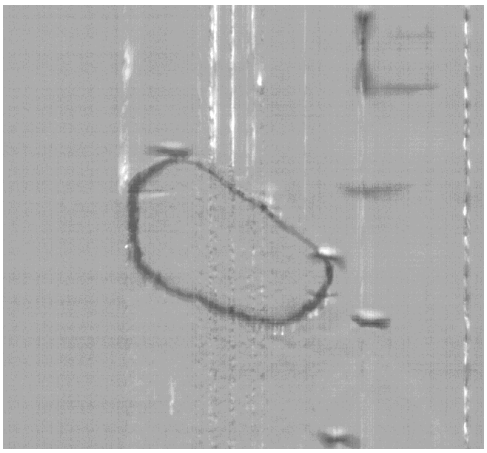

(b) Cleaned.

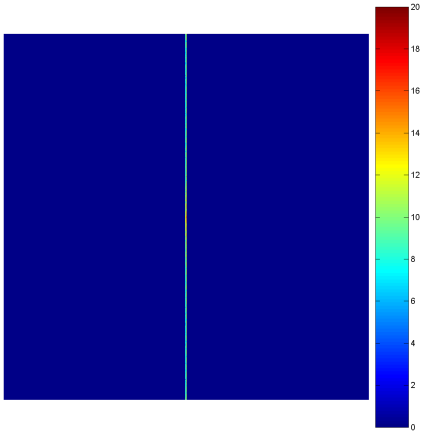

(c) FFT with the Chatter Data Band.

(d) Reconstruction of (c).

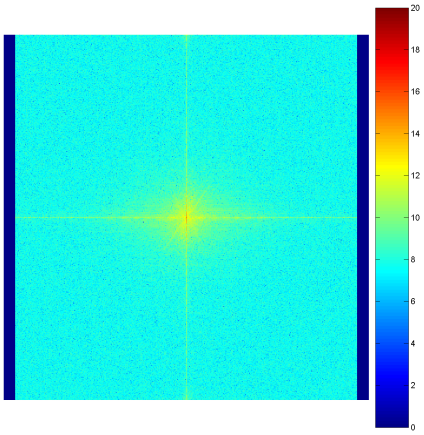

(e) FFT with the Whole Image Data Band.

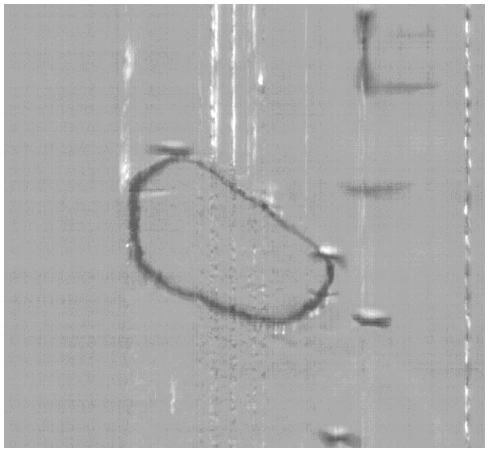

(f) Reconstruction of (e).

Figure 5.8: Image data collected while vibrating the knife at 10, 500 Hz frequency for the second test-case.

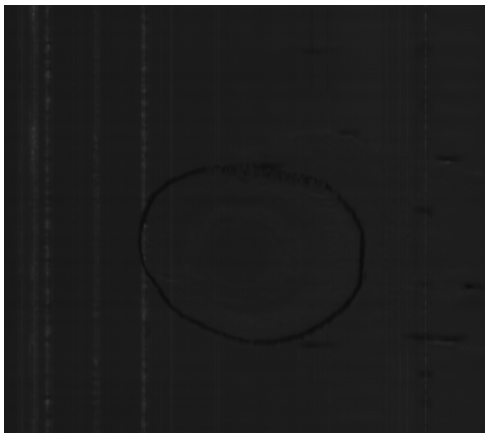

(a) Original.

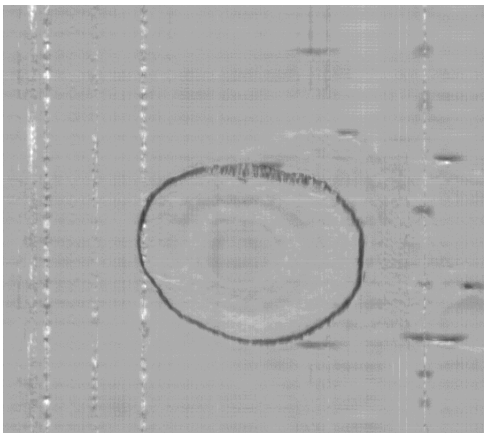

(b) Cleaned.

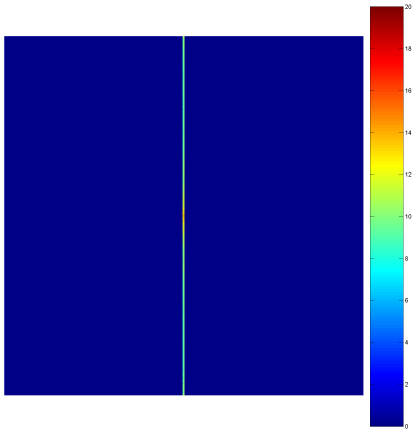

(c) FFT with the Chatter Data Band.

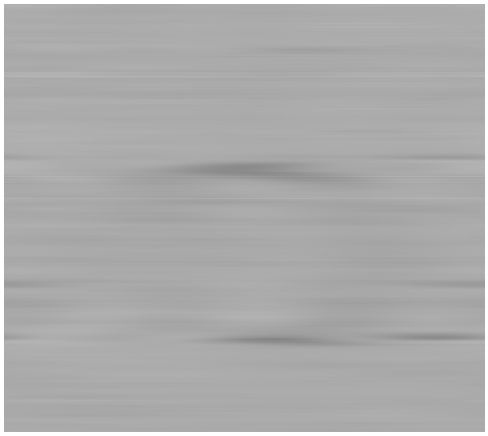

(d) Reconstruction of (c).

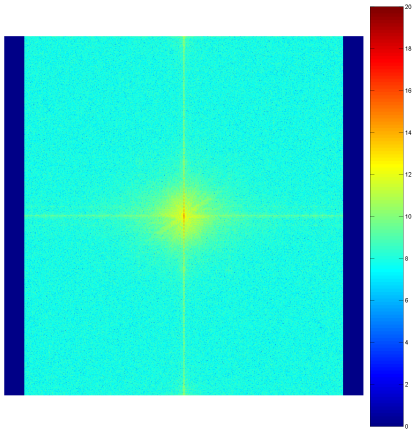

(e) FFT with the Whole Image Data Band.

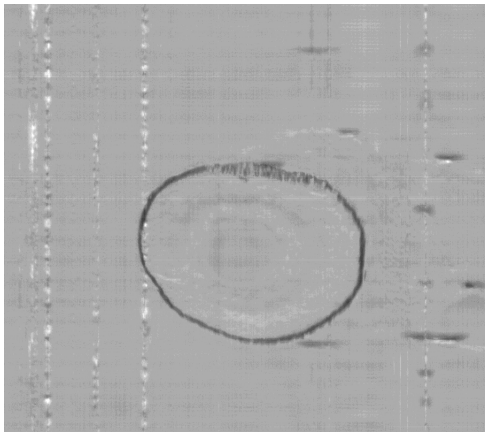

(f) Reconstruction of (e).

Figure 5.9: Image data collected while vibrating the knife at no frequency for the third test-case.

(a) Original.

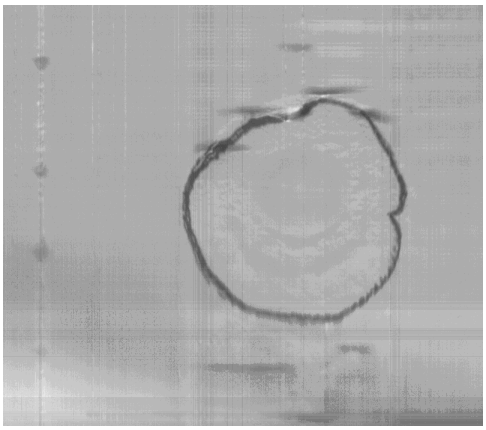

(b) Cleaned.

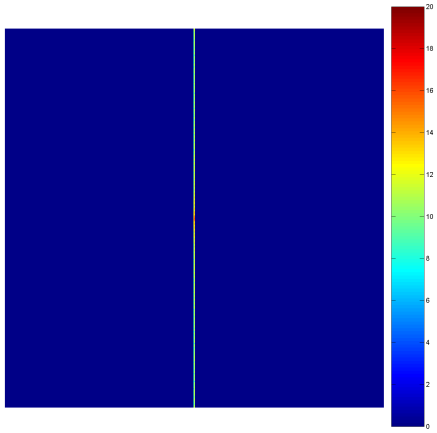

(c) FFT with the Chatter Data Band.

(d) Reconstruction of (c).

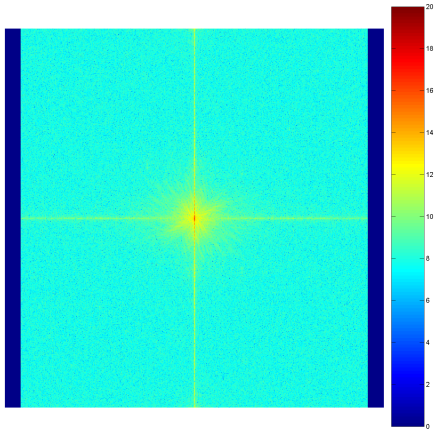

(e) FFT with the Whole Image Data Band.

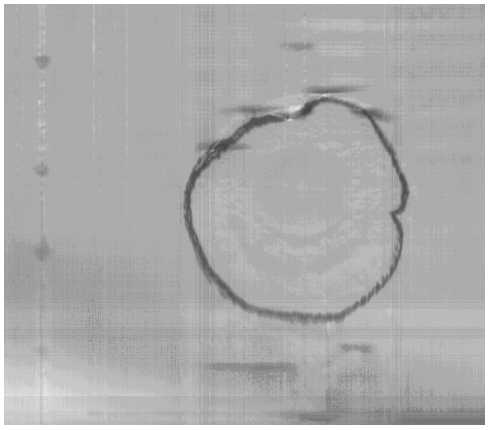

(f) Reconstruction of (e).

Figure 5.10: Image data collected while vibrating the knife at 2,500 Hz frequency for the third test-case.

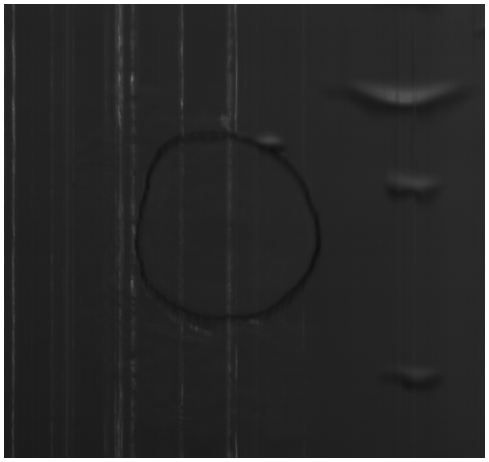

(a) Original.

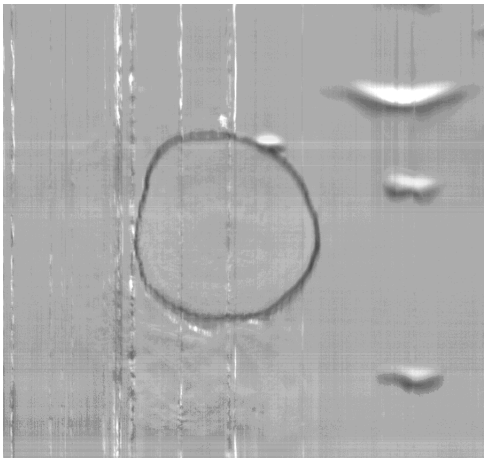

(b) Cleaned.

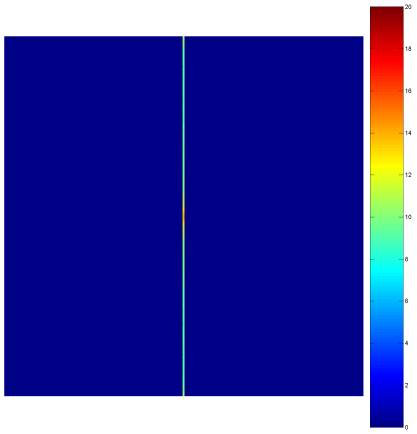

(c) FFT with the Chatter Data Band.

(d) Reconstruction of (c).

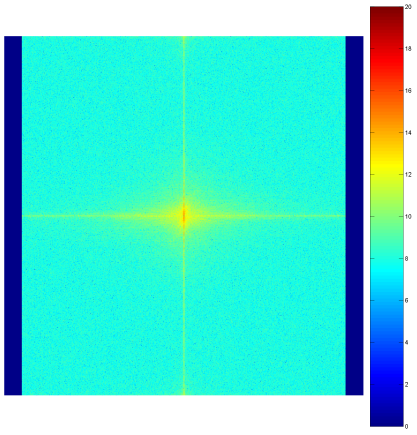

(e) FFT with the Whole Image Data Band.

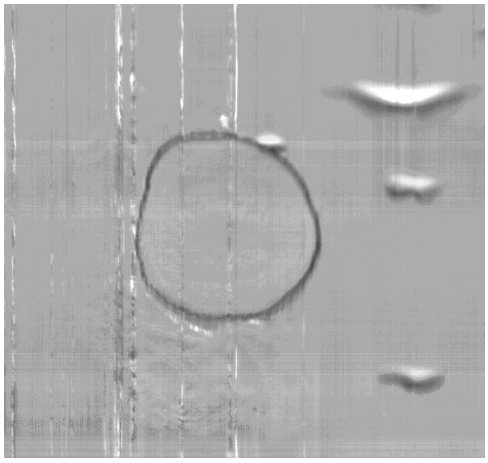

(f) Reconstruction of (e).

Figure 5.11: Image data collected while vibrating the knife at 7,500 Hz frequency for the third test-case.

(a) Original.

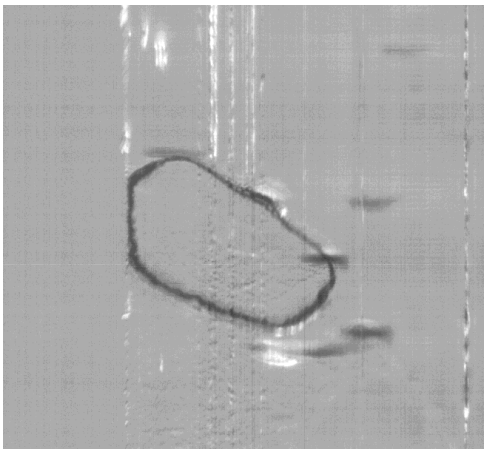

(b) Cleaned.

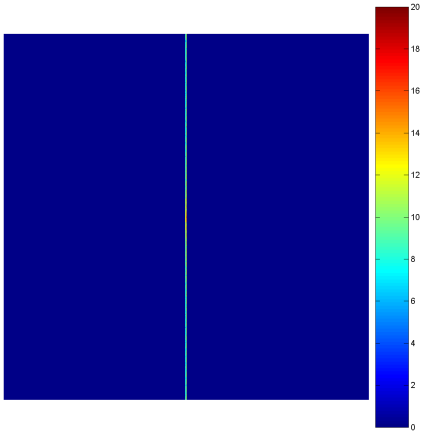

(c) FFT with the Chatter Data Band.

(d) Reconstruction of (c).

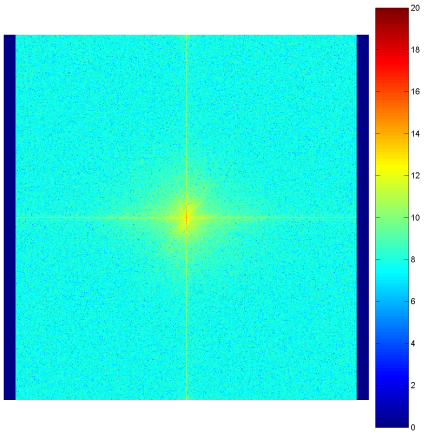

(e) FFT with the Whole Image Data Band.

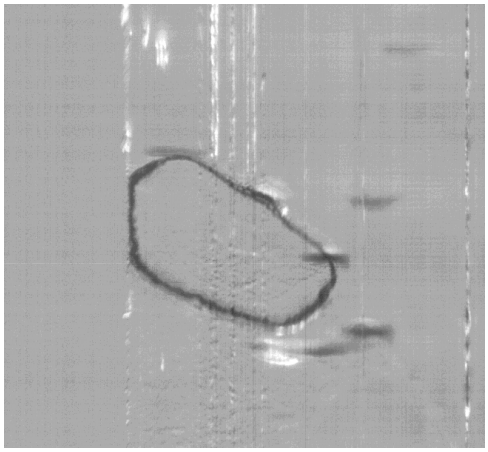

(f) Reconstruction of (e).

Figure 5.12: Image data collected while vibrating the knife at 10, 500 Hz frequency for the third test-case.

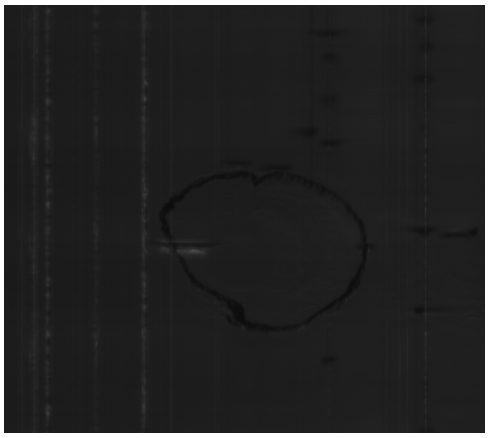

(a) Original.

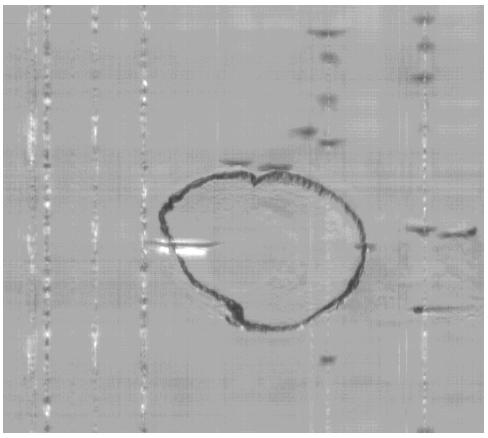

(b) Cleaned.

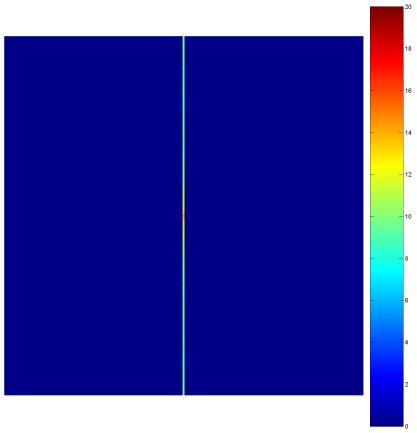

(c) FFT with the Chatter Data Band.

(d) Reconstruction of (c).

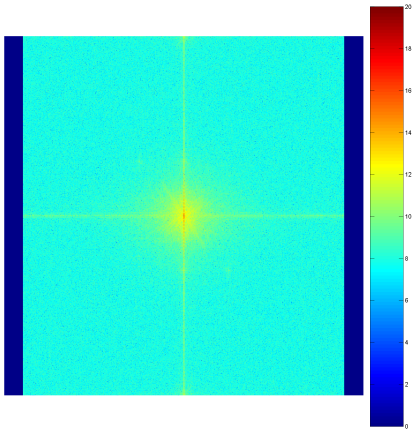

(e) FFT with the Whole Image Data Band.

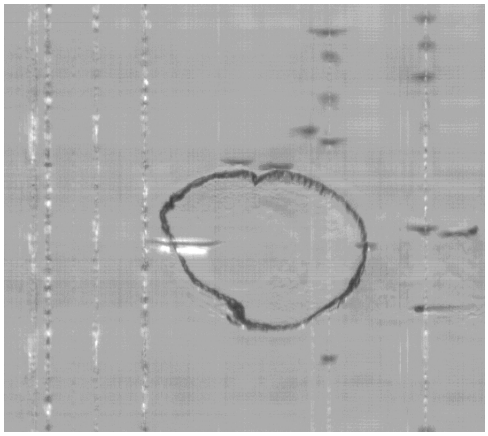

(f) Reconstruction of (e).

Figure 5.13: Image data collected while vibrating the knife at no frequency for the fourth test-case.

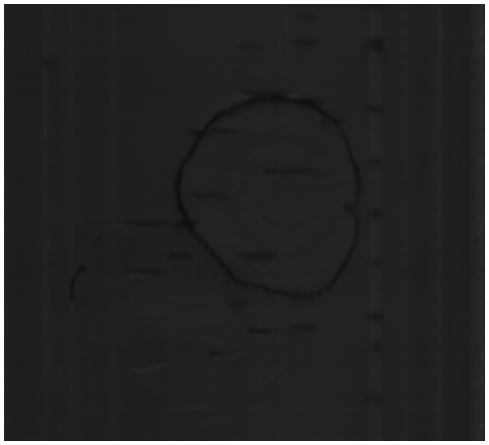

(a) Original.

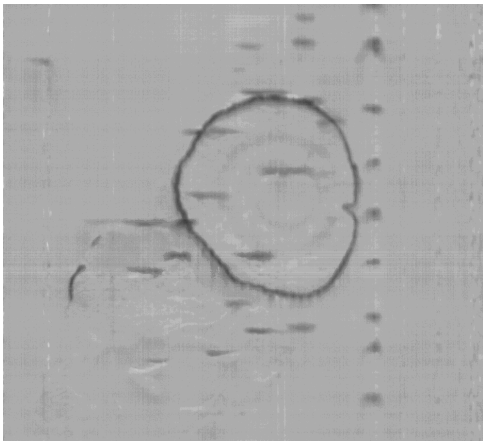

(b) Cleaned.

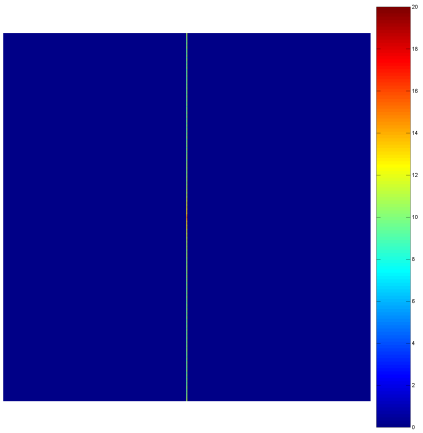

(c) FFT with the Chatter Data Band.

(d) Reconstruction of (c).

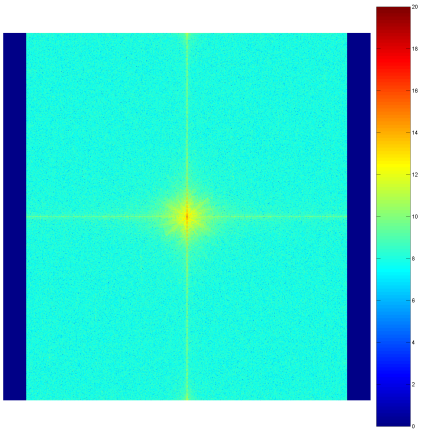

(e) FFT with the Whole Image Data Band.

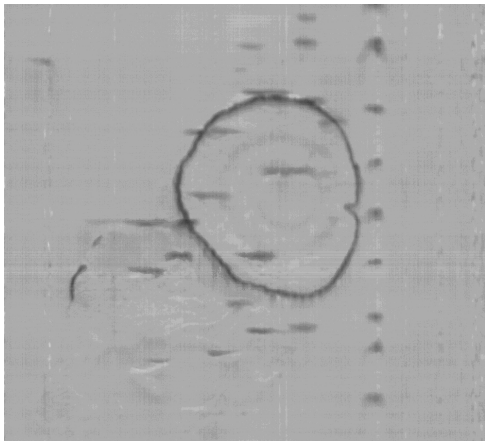

(f) Reconstruction of (e).

Figure 5.14: Image data collected while vibrating the knife at 2,500 Hz frequency for the fourth test-case.

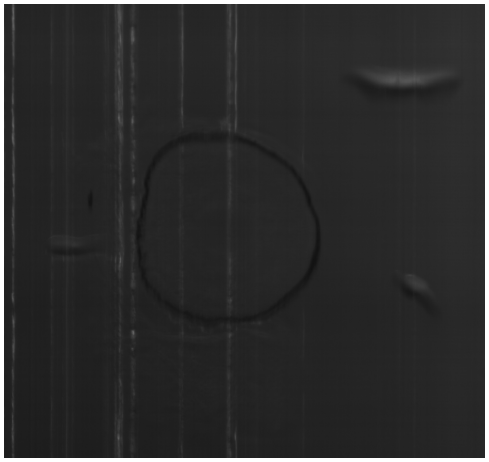

(a) Original.

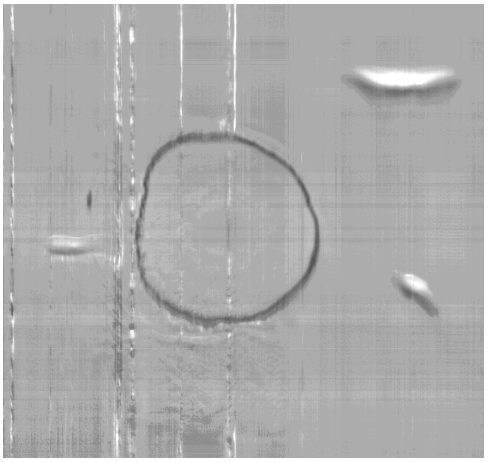

(b) Cleaned.

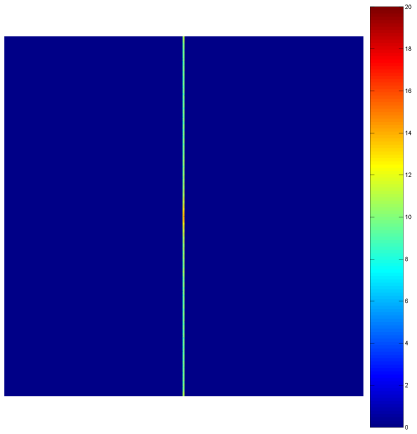

(c) FFT with the Chatter Data Band.

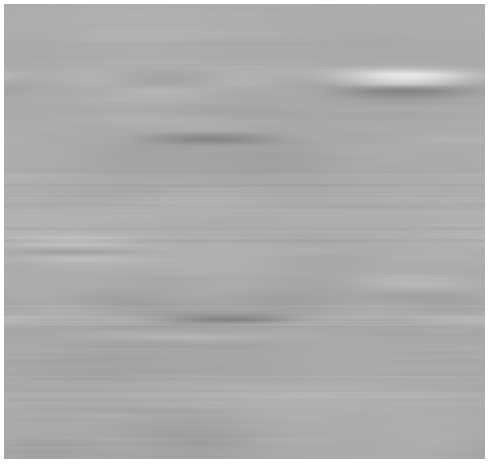

(d) Reconstruction of (c).

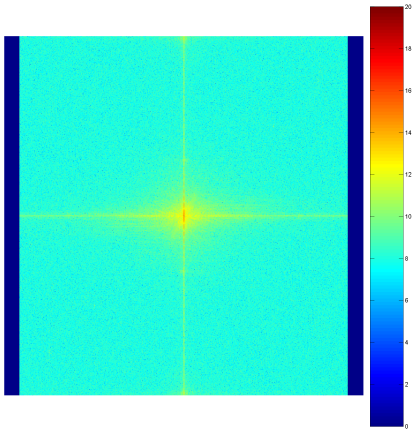

(e) FFT with the Whole Image Data Band.

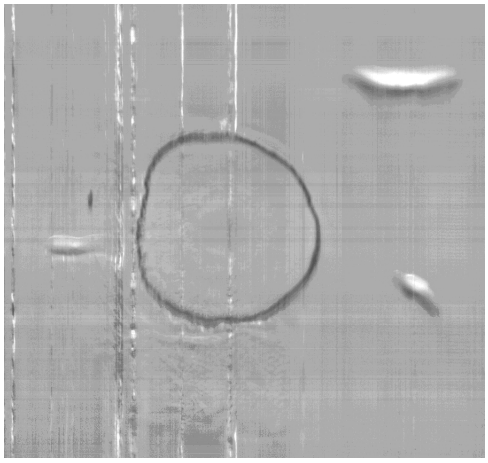

(f) Reconstruction of (e).

Figure 5.15: Image data collected while vibrating the knife at 7,500 Hz frequency for the fourth test-case.

	Leftmost unblocked column for chatter	Rightmost unblocked column for chatter	Leftmost unblocked column for all data	Rightmost unblocked column for all data	Width of chatter band	Width of data band	Ratio (Equation 4.8)
No Vibrations	-3	3	-400	400	5	799	0.006257822
2,500 Hz	-2	2	-367	367	3	733	0.004092769
7,500 Hz	-3	3	-406	406	5	811	0.006165228
10,500 Hz	-2	2	-304	304	3	607	0.004942339

Table 5.3: Results for test-case 3.

	Leftmost unblocked column for chatter	Rightmost unblocked column for chatter	Leftmost unblocked column for all data	Rightmost unblocked column for all data	Width of chatter band	Width of data band	Ratio (Equation 4.8)
No Vibrations	-3	3	-403	403	5	805	0.00621118
2,500 Hz	-2	2	-433	433	3	865	0.003468208
7,500 Hz	-3	3	-412	412	5	823	0.006075334
10,500 Hz	-2	2	-311	311	3	621	0.004830918

Table 5.4: Results for test-case 4.

Looking at the results, it is evident that the image data obtained under the condition of vibrating the knife at 2,500 Hz has the lowest ratio, which means that it has the lowest proportion of frequencies that are devoted exclusively to the chatter. All the zebra-fish samples used were stained using the same batch of nissl ink, so the hardness of the nissl ink was uniform among all the samples, and thus did not contribute to the difference.

The ratios from each experimental condition were statistically analyzed using ANOVA1 function of MATLAB, to determine if the results were obtained just by chance. The p-value from the analysis was 0.0000681, indicating that the experimental results were not a product of chance.

(a) Original.

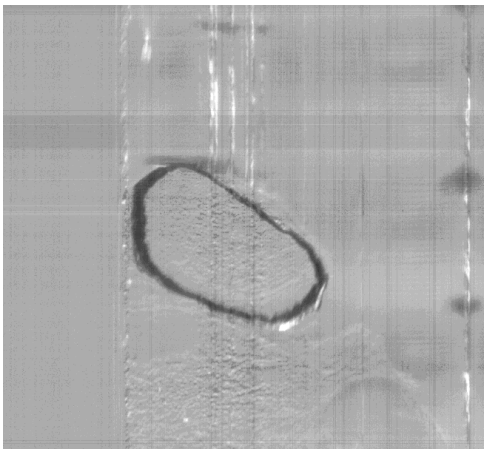

(b) Cleaned.

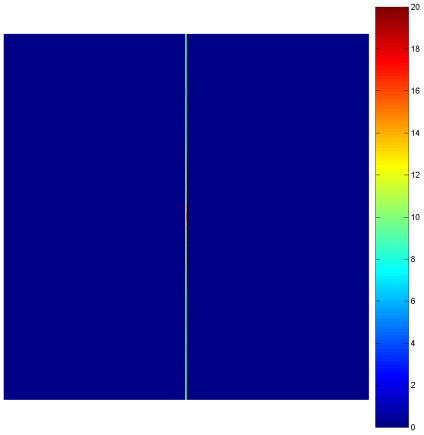

(c) FFT with the Chatter Data Band.

(d) Reconstruction of (c).

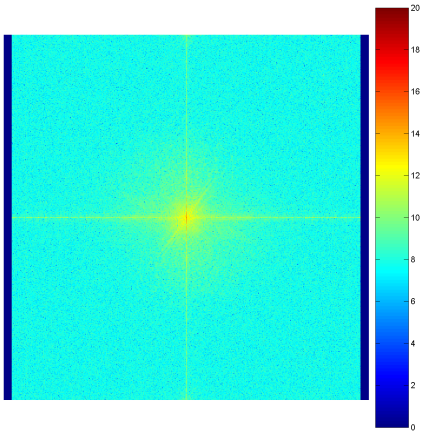

(e) FFT with the Whole Image Data Band.

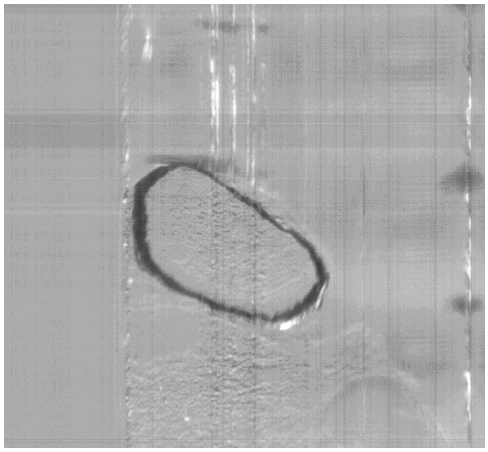

(f) Reconstruction of (e).

Figure 5.16: Image data collected while vibrating the knife at 10, 500 Hz frequency for the fourth test-case.

	Test-Case 1	Test-Case 2	Test-Case 3	Test-Case 4	Average
No Vibrations	0.006257822	0.006289308	0.006257822	0.00621118	0.006254033
2,500 Hz	0.005524862	0.004195804	0.004092769	0.003468208	0.004320411
7,500 Hz	0.00622665	0.006337136	0.006165228	0.006075334	0.006201087
10,500 Hz	0.004942339	0.004926108	0.004942339	0.004830918	0.004910426

Table 5.5: Average of the results for all the 4 test-cases.

5.4 Bias in Determining the Chatter Bandwidth

The fact that determining the chatter bandwidth is subjective demands a way to test the accuracy of the manually selected chatter bandwidths. Three different experts were asked to determine the chatter bandwidths of the images in the test-cases. From the entire 16-image set (from 4 test cases), each image's FFT was reconstructed with chatter-bandwidths of 1, 3, 5, 7, and 9. The reconstructions were stopped at a chatter-bandwidth of 9 because in all cases, the reconstructions obtained at a chatter-bandwidth of 9 had an obvious object present in them.

Three experts were shown such reconstructions of all the 16 test-case images. They were asked to complete the task described as follows:
"Every test case has images acquired from 4 different experimental conditions: No vibrations to the knife, and vibrations of 2500 Hz, 7500 Hz, and 10,500 Hz.

Please go to each subfolder in the test cases, and look at the images in order: a, b, c, d, and e. As you go through these images in order, you'll eventually see an image with some hint of the object (a rough circle). Write down the filename of the image before this image with the object. So if you look at a, then b, and then you see some hint of an object in c, note down b in the 'Opinion.txt' file provided."

Here, images with name 'a' were a reconstruction obtained at a chatter-bandwidth

of 1, 'b' at a chatter-bandwidth of 3, 'c' at a chatter-bandwidth of 5, 'd' at a chatter-bandwidth of 7, and 'e' at a chatter-bandwidth of 9. To prevent any kind of bias, the experts were not given this information.

Once this data was acquired, it was compared against my determinations of chatter-bandwidths. Tables 5.6, 5.7, 5.8, and 5.9 contain the results:

	Expert 1	**Expert 2**	**Expert 3**	**My Answer**	**Number of Matches**
No Frequency	5	5	5	5	3
2,500 Hz	3	3	7	5	0
7,500 Hz	3	3	7	5	0
10,500 Hz	3	3	5	3	2

Table 5.6: Determination of Chatter-Bandwidths for Images in Test-Case 1.

	Expert 1	**Expert 2**	**Expert 3**	**My Answer**	**Number of Matches**
No Frequency	5	3	5	5	2
2,500 Hz	3	3	7	3	2
7,500 Hz	5	3	5	5	2
10,500 Hz	5	3	7	3	1

Table 5.7: Determination of Chatter-Bandwidths for Images in Test-Case 2.

As it can be seen from the tables, my determinations agree with at least 1 of the experts' determinations in 11 out of 16 cases. However, if each of these other chatter-bandwidths are used to calculate the ratios (just like my determinations were used in calculating the rations in tables 5.1, 5.2, 5.3, and 5.4), and the average is taken, we get the results in table 5.10:

	Expert 1	Expert 2	Expert 3	My Answer	Number of Matches
No Frequency	5	3	7	5	1
2,500 Hz	7	3	5	3	1
7,500 Hz	5	3	7	5	1
10,500 Hz	5	3	5	3	1

Table 5.8: Determination of Chatter-Bandwidths for Images in Test-Case 3.

	Expert 1	Expert 2	Expert 3	My Answer	Number of Matches
No Frequency	3	3	7	5	0
2,500 Hz	5	1	5	3	0
7,500 Hz	3	3	7	5	0
10,500 Hz	3	3	5	3	2

Table 5.9: Determination of Chatter-Bandwidths for Images in Test-Case 4.

We can see from the results that 2,500 Hz is, on average, still the frequency that reduces the knife chatter the most, which matches with the results obtained using my determinations of chatter-bandwidths. The results from table 5.10 were statistically analyzed using the ANOVA1 function of MATLAB, and the p-value from the analysis was 0.841. It is high unlike the p-value for table 5.5, which is 0.0000681. I think that this contradiction is because of the fact that we are trying to measure something subjective.

	Expert 1	Expert 2	Expert 3	Average Ratio
No Frequency	0.005632915	0.004378202	0.007500933	0.00583735
2,500 Hz	0.005710216	0.00318989	0.007531661	0.005477256
7,500 Hz	0.004970889	0.003720652	0.008047808	0.005579783
10,500 Hz	0.006555168	0.004910426	0.009005062	0.006823552

Table 5.10: Average of the ratios obtained from the chatter-bandwidths determined by the experts.

6. ISLOATING CHATTER FROM THE OBJECT

Knife chatter is undesirable but unfortunately, knife chatter is unavoidable. The good news is that it is possible to reduce the knife chatter using a technique described in this chapter. Knife chatter appearing in the images obtained using the KESM is hard to distinguish from the object algorithmically but FFTs can help us to some degree in separating out the chatter. A vertical band in the center of the FFTs of a typical image obtained using the KESM contains information exclusively about the knife chatter. The rest of the FFT contains information about both, the object and the chatter. Bandpass-filtering the image does not remove the chatter though. The chatter bandwidth portion of the FFT can be blocked out, along with the region beyond the bounds of total image data bandwidth. The reconstructions of such bandpass-filtered FFTs still contain chatter. Figure 6.1 shows an example. Some amount of chatter is removed, but not all. However, there is an alternate way to remove chatter.

A reconstruction of the FFT of the original image with everything blocked out except for the chatter band contains streaks where there is chatter in the original image. The streaks are not the same shape and size as the chatter but they are in the same location. If the reconstructed image is intersected (explained in the next paragraph) with the original image, the result would have the chatter but not the object.

An intersection between two grayscale images here is defined as keeping the corresponding pixels in the two images that have the same grayscale value, and reducing the other pixels to a zero value. Intersection between the reconstruction and the original image cannot be done directly since the streaks in the reconstruction and

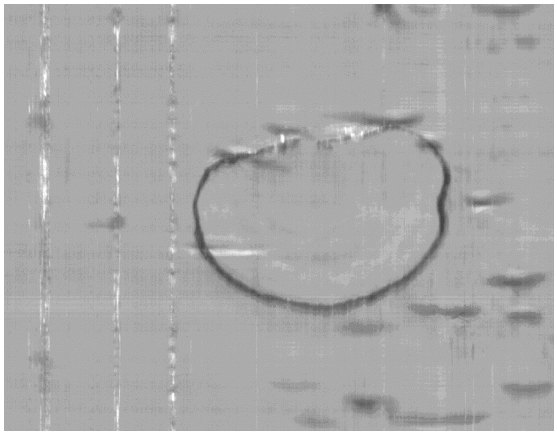

(a) The original image. The knife was not vibrated to acquire this image. It shows a zebra-fish embryo eye.

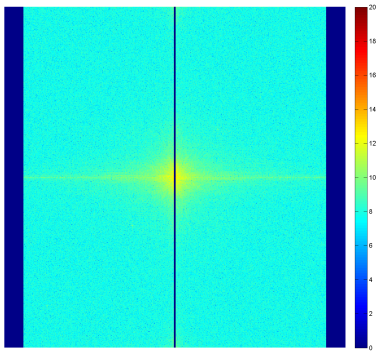

(b) A bandpass-filtered FFT of the image in (a). The DC component of the FFT was retained to maintain the brightness of the reconstruction.

(c) A reconstruction of the bandpass-filtered FFT in (b).

Figure 6.1: An example demonstrating bandpass filtering.

the chatter in the original image have different grayscale values. However, if we threshold both the images so that any pixel is either 0 (black) or 255 (white), it is possible to do a simple intersection between the processed images.

To illustrate this idea, consider the image shown in Figure 6.2. It shows an image acquired during the sectioning of a zebra-fish eye. The image contains some knife chatter. Figure 6.4 shows the reconstruction after 5 columns in the center of the FFT of the source image were blocked out. By applying a threshold of 152 (a pixel above this value is considered 0 and below this value is considered 255) on the reconstruction, the resulting image contains just the streaks as shown in figure 6.5. Applying a similar threshold to the original image, we get the image in figure 6.3. Now, we can easily perform an intersection between the two filtered images. The result of the intersection is shown in figure 6.6. Figure 6.7 shows the original image and the intersection side-by-side. As it can be seen, the intersection contains mostly the knife chatter and almost no object.

This technique can be significantly helpful in removing chatter from the KESM images. The only limitation is that determining the threshold is done manually. It would be desirable to have an algorithm decide the threshold.

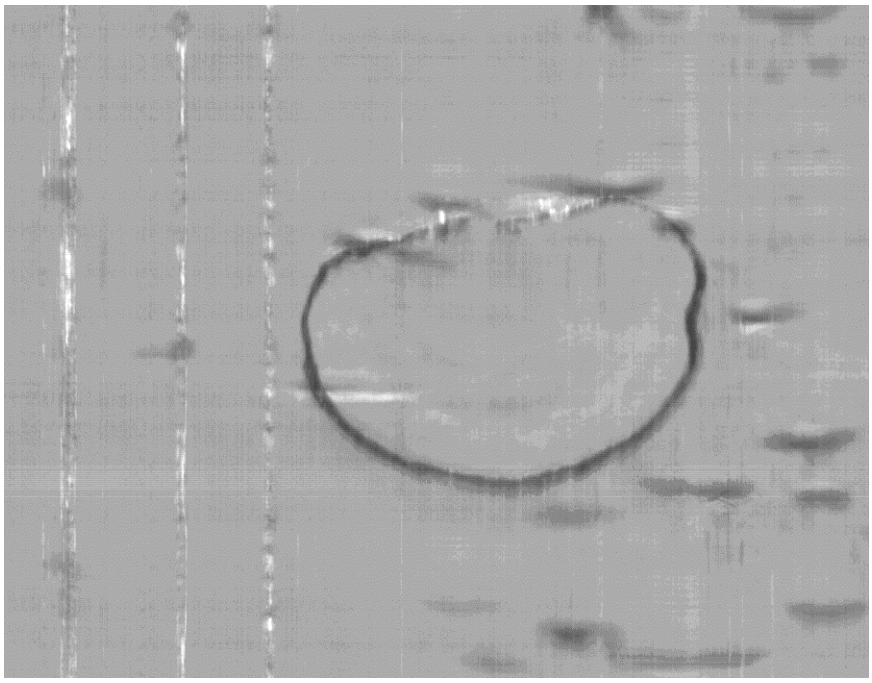

Figure 6.2: A sample image from the KESM data set. This was acquired when sectioning a zebra-fish. The knife was fed no input frequency.

Figure 6.3: Figure 6.2 with a threshold of 143.

Figure 6.4: Figure 6.2 reconstructed after blocking out everything in its FFT except for 5 columns in the center.

Figure 6.5: Figure 6.4 with a threshold of 152.

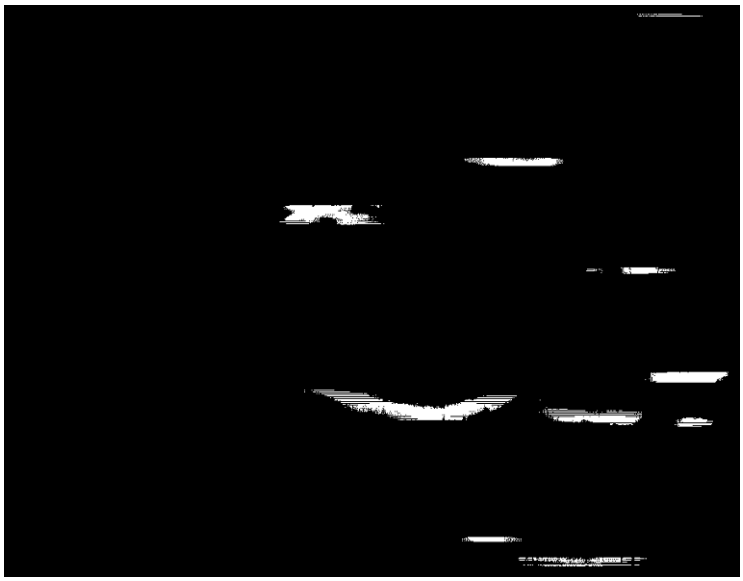

Figure 6.6: Figure 6.5 and Figure 6.3 intersected. Most of the chatter in the source image is singled out.

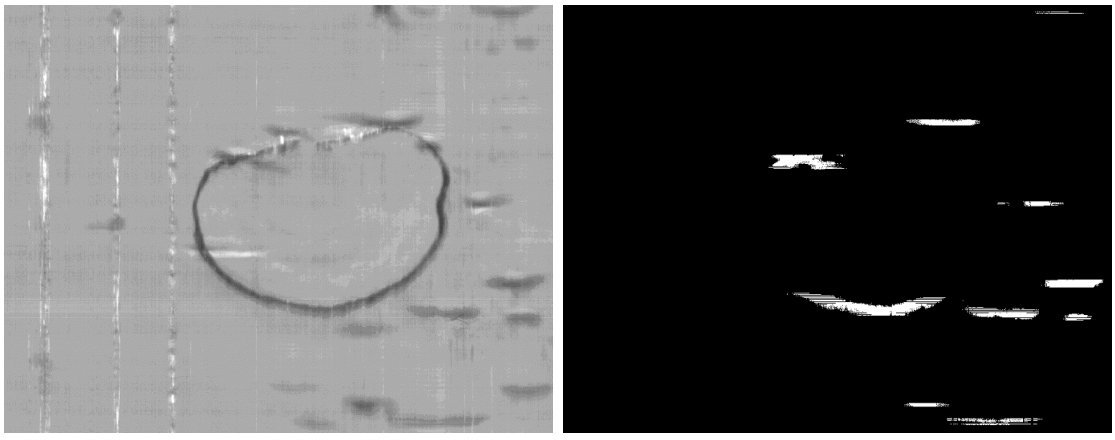

(a) (b)

Figure 6.7: Comparing the source image and the extracted chatter.

7. DISCUSSION AND CONCLUSION

One of the main contributions of this thesis was to show that knife chatter in the KESM images can be quantified as the percentage of the total image data bandwidth taken up exclusively by chatter.

Another contribution was the discovery that sectioning of zebra-fish embryos using a vibrating knife under different experimental conditions (different oscillating frequencies used for the knife) suggests that among the four conditions of no vibrations, 2,500 Hz, 7,500 Hz, and 10,500 Hz, the image data obtained at 2,500 Hz contains the least amount of knife chatter as calculated by the metric described in the previous section.

There may be other frequencies that have even a lower amount of knife chatter. This result provides an important guideline that using a vibrating knife does reduce the knife chatter. Further work can be done to find out the optimal frequency, the frequency at which the knife chatter in the images is the lowest possible.

Knife chatter is undesirable, but unfortunately, knife chatter is always going to be present in the KESM images because eliminating the knife's vibrations caused by environmental factors is generally very difficult. The good news is that it is possible to reduce the knife chatter using the techniques described in this thesis.

Furthermore, isolating knife chatter is also possible using the method shown in Chapter 6. The algorithm proposed has to be improved upon so that it is fully automated, e.g., automated selection of thresholds.

REFERENCES

[1] Guntupalli, Jyothi Swaroop. "Physical Sectioning in 3D Biological Microscopy". Diss. Texas A&M University, 2007.

[2] McCormick, B.H. "Brain Tissue Scanner Enables Brain Microstructure Surveys". Neurocomputing, 44-46:1113-1118. 2002.

[3] Mayerich, David, Bruce H. McCormick, and John Keyser. "Noise and Artifact Removal in Knife-Edge Scanning Microscopy".Biomedical Imaging: From Nano to Macro, 2007. ISBI 2007. 4th IEEE International Symposium on. IEEE, 2007.

[4] R. Phillips. "Diamond Knife Ultra Microtomy of Metals and the Structure of Microtomed Sections". British Journal of Applied Physics, vol. 12, pp. 554-558. October 1961.

[5] Marian Wiercigroch and Erhan Budak. "Sources of Nonlinearities, Chatter Generation and Suppression in Metal Cutting". Philosophical Transactions of the Royal Society A: Mathematical, Physical and Engineering Sciences, vol. 359, no. 1781, pp. 663-693. April 2001.

[6] B. H. McCormick, D. M. Mayerich, and M. Wiercigroch. "Nanomachining for High-Resolution Scanning of Mammalian Brain Microstructure". Proceedings, 11th International Conference on Fracture, Turin, Italy. March 2005.

[7] Sohail A. Dianat. "E-Study Guide For: Advanced Linear Algebra for Engineers". Cram101. N.p., n.d. June 2014.

[8] D. Studer, H. Gnaegi. "Minimal Compression of Ultrathin Sections with Use of an Oscillating Diamond Knife". Journal of Microscopy, vol. 197, no. 1, pp. 94-100. 2000.

[9] D. M. Mayerich. “Acquisition and Reconstruction of Brain Tissue Using Knife-Edge Scanning Microscope”. M.S. Thesis, Dept of Computer Science, Texas A&M University. 2003.

[10] Mayerich, David, et al.“Fast Macro-Scale Transmission Imaging of Microvascular Networks Using KESM”. Biomedical Optics Express 2.10 (2011): 2888-2896.

[11] Chung, Ji Ryang, et al.“Multiscale Exploration of Mouse Brain Microstructures Using the Knife-Edge Scanning Microscope Brain Atlas”. Frontiers in Neuroinformatics 5 (2011).

[12] Mayerich, David, L. Abbott, and B. McCormick.“Knife-Edge Scanning Microscopy for Imaging and Reconstruction of Three-Dimensional Anatomical Structures of the Mouse Brain”. Journal of Microscopy 231.1 (2008): 134-143.

[13] Gu, Hongyan, et al.“Controlled Chattering-a New ‘Cutting-Edge’ Technology for Nanofabrication”. Nanotechnology 21.35 (2010): 355302.

[14] Lyons, Richard. G. G.“Understanding Digital Signal Processing”. Third Edition. Prentice Hall, (2010).

[15] Annadurai, S., and R.Shanmugalakshmi.“Fundamentals of Digital Image Processing”. Pearson Education India, (2006).

[16] D. M. Mayerich.“Acquisition and Reconstruction of Brain Tissue Using Knife-Edge Scanning Microscope”. M.S. Thesis, Dept of Computer Science, Texas A&M University. 2003.

[17] Choe, Yoonsuck.“Physical Sectioning Microscopy”. In Dieter Jaeger and Ranu Jung, editors, Encyclopedia of Computational Neuroscience. Springer, Berlin, 1st edition, 2014. In press.

[18] Hayworth, K. J., et al."Automating the Collection of Ultrathin Serial Sections for Large Volume TEM Reconstructions". Microscopy and Microanalysis 12.S02 (2006): 86-87.

[19] Micheva, Kristina D., and Stephen J. Smith."Array Tomography: a New Tool for Imaging the Molecular Architecture and Ultrastructure of Neural Circuits". Neuron 55.1 (2007): 25-36.